universität wien

MASTERARBEIT / MASTER'S THESIS

Titel der Masterarbeit / Title of the Master's Thesis

Development and evaluation of daily increments in *Chondrostoma nasus* during early ontogeny

verfasst von / submitted by

Reinhard Krusch BSc

angestrebter akademischer Grad / in partial fulfilment of the requirements for the degree of

Master of Science (MSc)

Wien, 2016

Studienkennzahl lt. Studienblatt / degree programme code as it appears on the student record sheet:	A 066 833
Studienrichtung lt. Studienblatt / degree programme as it appears on the student record sheet:	Masterstudium Ecology and Ecosystems UG2002
Betreut von / Supervisor:	Ao. Univ. Prof. Dr. Hubert Keckeis
Mitbetreut von / Co-Supervisor:	

Table of Contents

Abstract

This study focuses on the development and validation of daily growth increments in otoliths of embryonic and larval life stages of the nase (*Chondrostoma nasus*). Individuals used for the study were reared in flow-through tanks at two different temperatures (warm: 16.7° ± 1.1; cold: 11.4° ± 0.9). Samples of 10 individuals from each temperature were taken in daily intervals starting at fertilization of the eggs and continuing for 47 days for cold- and 90 days for warm-reared individuals. For every individual, total size was measured and sagittae and lapilli otoliths were extracted and fixed in artificial resin on microscope slides. These slides were used to measure otolith size (diameter) and for age determination, based on microstructures, under a light microscope. The main focus of the structure analysis was on verifying and counting daily rings. Additionally, otoliths were examined for distinguishable and recurring structures and their link to developmental events. For aging based on daily rings, the time of first increment deposition had to be established. At both temperatures and for both types of otoliths, 2 rings were present at the day of hatching. A circadian rhythm of matter deposition was verified, and the usefulness of the resulting ring structures for age estimations, after implementing a procedure proposed by Campana (1992), showed high accuracy. The accuracy of age determination using ring counts was compared to age estimations based on individual size or otolith size measurements. Both these parameters correlated highly significantly with age, as did the ring counts. Total length and otolith diameters both showed a strong temperature dependency, which was not present in daily ring deposition. The results of this study enable estimating the age of wild caught larvae of nase, determining the range of their hatching times, as well as back-calculating the growth of released and recaptured larva on a daily basis.

Key words

Otoliths, early stages, *Chondrostoma nasus*, growth, daily ring formation, otolith diameter, age determination, temperature,

Zusammenfassung

Die Arbeit legt den Fokus auf die Validierung und Entwicklung täglicher Wachstumsinkremente in den Otolithen von Embryonal- und Larvalstadien der Nase (*Chondrostoma nasus)*. Die Aufzucht der verwendeten Individuen erfolgte in durchflossenen Wannen bei zwei verschiedenen Temperaturen (warm: 16.7° ± 1.1; kalt: 11.4° ± 0.9). Proben von 10 Individuen aus beiden Temperaturen wurden in täglichen Intervallen genommen, beginnend mit der Befruchtung der Eier, über einen Zeitraum von 47 Tagen (kalt) und 90 Tagen (warm). Von jedem Individuum wurde die Totallänge gemessen sowie Sagittae und Lapilli Otolithen entnommen, welche dann auf Objektträgern in Kunstharz fixiert wurden. Die Otolithen wurden unter einem Mikroskop vermessen (Durchmesser) und zur Altersbestimmung anhand von Mikrostrukturen verwendet. Der Hauptfokus der Strukturanalyse lag auf der Verifikation und Zählung von Tagesringen. Zusätzlich wurden die Otolithen auf wiederkehrende und erkennbare Strukturen untersucht, sowie deren Verbindung zu Entwicklungsereignissen. Zur Altersbestimmung anhand von Tagesringen wurde der Zeitpunkt der erstmaligen Entstehung ermittelt. In beiden Temperaturen und für beide verwendeten Paare von Otolithen waren am Tag des Schlüpfens bereits 2 Ringe vorhanden. Ein zirkadianer Rhythmus der Materialablagerung konnte verifiziert werden und Altersbestimmungen anhand der resultierenden Ringstrukturen, nach einer Methode vorgeschlagen von Campana (1992), zeigten eine hohe Genauigkeit. Die Genauigkeit der Altersbestimmung anhand von Ringzählungen wurde mit Altersschätzungen basierend auf Länge von Individuen oder Durchmesser von Otolithen verglichen. Alle diese Parameter korrelierten hoch signifikant mit dem Alter des Individuums. Länge der Larven sowie auch Durchmesser der Otolithen zeigten eine starke Abhängigkeit von der Umgebungstemperatur, diese hatte jedoch keinen Einfluss auf die Entstehung von Tagesringen. Die Ergebnisse dieser Studie ermöglichen eine Schätzung des Alters von wild gefangenen Nasenlarven, daraus eine Festlegung ihrer Schlupfzeiten sowie eine Rückberechnung des Wachstums von Larven aus Wiederfangexperimenten.

Schlüsselwörter

Otolithen, Frühe Entwicklungsstadien, *Chondrostoma nasus*, Entstehung von Tagesringen, Otolithen Durchmesser, Altersbestimmung, Temperatur

Introduction

The process of aging fish has been a field of interest to fisheries and regulatory bodies for many decades and its importance continues to grow. This is in part related to the ever-increasing challenge of maintaining stable populations of edible or protected species. Recent trends in inland fisheries management have attempted to address problems created by societal development and sought to improve the aquatic environment for biodiversity (Arlinghaus *et al.* 2002; Cowx 2004). This is a necessary step in fulfilling the obligations of recent conventions and directives (e.g. European Water Framework Directive 200/60/EEC), which aim to protect and improve water quality (Arlinghaus *et al.* 2002). These water quality improvements have rarely been successful at substantially protecting and enhancing freshwater fish populations (Raat 2001; Souchon and Keith 2001). Fish species diversity depends more strongly on rehabilitating habitat structure and maintaining lateral and longitudinal connectivity (e.g. Lucas and Marmulla 2000; Wolter 2001; Collares-Pereira *et al.* 2002; Arlinghaus *et al.* 2002) than on water quality improvements. This leads to the need to identify individual species' requirements in spawning grounds and nursery habitats. A useful tool in the search for already existing habitats that fulfil these requirements is the ability to age wild-caught larvae and juvenile fish as accurately as possible. To fisheries biologists, otoliths are a key structure for understanding the life of fish and fish populations (Campana 2004). They form the basis for most age-structured analyses of fish populations around the world (Summerfelt and Hall 1987; Secor *et al.* 1995; Fossum *et al.* 2000). World-wide the number of counts exceeded 2 million fish per year in 2008 (Fowler 2009), a significant increase from an estimated 800 000 in 1999 (Campana and Thorrold 2001). Almost all these counts were annual counts on adult marine fish.

In addition to the annual rings on otoliths, much smaller structures are generated daily and visible only under a microscope (Pannella 1971). These daily increments of otoliths are the result of an alternating deposition of two different materials on the otolith surface during one day. These two materials have two distinct achromatic colorations, with $CaCO_3$ in a crystalline structure forming a white band, and Otolin, which serves as a matrix protein, forming dark, nearly black rings. These daily accretions are visible when examining a cross section of an

otolith under a microscope. They form in the first year of life and record daily age and growth patterns in surprising, albeit microscopic, detail (Campana and Neilson 1985).

One feature of daily otolith growth is that the circadian rhythm shown is constant, without external “pacemakers” such as a diurnal light-dark cycle (Whitmore *et al.,* 1998). The explanation of this phenomenon is that the accretion of materials on the otolith surface is controlled by the endocrine system and is coupled to the biological or “inner” clock of fish (Kulczykowska *et al.,* 2010). In most organisms, ranging in complexity from cyanobacteria to vertebrates, this regulatory system is under genetic control. In addition to other time-sensitive physiological and behavioral processes, it also controls the deposition of materials on the otolith surface (Kulczykowska *et al.,* 2010). The daily rhythm of otolith growth is further stabilized by the morphological properties of the vertebrate inner ear. The otoliths are located in fluid-filled sacs termed utricles. They form a controlled, closed system as far as the chemical composition of the enclosed endolymph is concerned. This closed system prevents changes in the daily deposition rhythm due to potential fluctuations in the chemical composition of the surrounding habitat, which are otherwise known to influence the physiological development and growth rates of fish. $CaCO_3$ and matrix proteins are produced directly in the utricle walls (Mugiya 1987). For otolith deposition rates, this also means that the concentrations in the endolymph can be strictly controlled. These concentrations change over a day and are almost antiphasal, with a diurnal shift from $CaCO_3$ to protein deposition (Mugiya 1987). This corresponds to and verifies observations of daily accretions in the otoliths of *Chondrostoma nasus* in this study and others (Schludermann *et al.,* 2009). One factor not regulated in the utricles and known to influence daily ring formation on otoliths are temperature fluctuations, which have been related to changes in increment periodicity, width, and optical density (Campana and Neilson, 1985; Mosegaard *et al.*, 1987; Brothers, 1990; Volk *et al.*, 1990, 1994; Munk *et al.*, 1993). An artificial temperature drop of 2 to 5 °C over several days is widely used, mostly for salmonids, to establish a visible structure corresponding to a certain time. That time is then used as a marker in recapture experiments (Volk and Hagen, 2001). A naturally occurring temperature drop or rise of this magnitude over a short time is an event that can be easily traced using environmental data. This can create a visible marker for any age estimations related to a specific date.
The separation of outside influences, coupled with the very early emergence of otoliths and

the fact that they are never reabsorbed, makes them a prime source of information for all aging with fish larvae and juveniles.

The present study focuses on the very early developmental stages of *C. nasus,* a formerly dominant fish in many European rivers but now endangered in most European countries (Lelek 1987). It has become a target for research and applied studies in river ecology and restoration (Keckeis *et al.* 2000). This study verifies the circadian rhythm of daily ring depositions in otoliths and defines the accuracy with which they can be used to estimate larval age in days (e.g., Pannella 1971; Miller and Storck 1982; Barkman and Bengtson 1987; Parsons and Peters 1989; Karakiri and Westerhagen 1989). This includes verifying the first appearance of otoliths as well as the first increment deposition. The present study also examines the extent to which major developmental events during early development (i.e. hatching, beginning of external feeding) can be related to otolith structures (Marshall and Parker 1982; Kristensen *et al.,* 2008; Joh *et al.,* 2014). The data set of otolith and individual sizes was also used to investigate the relationship between otolith size and individual size. The role of the two different temperatures in otolith and fish growth was calculated and a potential influence of temperature on increment periodicity was investigated (Moosegaard *et al.,* 1988; Günther *et al.,* 2012; Otterlei *et al.,* 2002).

Material and Methods

Stripping and culturing of fish

Spawners of nase carps (*Chondrostoma nasus*) of both sexes were caught by means of electrofishing during their spawning migration in the Schwechat River, a tributary of the Danube east of Vienna, on 22 and 23 March 2012. The fish were hand-stripped and the eggs fertilized (dry method) promiscuously (1 female and 3-5 males). After this procedure, the parental fish were then transported back to the river and released at the same place where they were caught. Approx. 216,000 eggs were placed in 4 flow-through tanks – 40 cm wide and 220 cm long – holding 150 l water (Figure 1). A constant through-flow of filtered and oxygen-saturated (100% ± 10%) water was maintained. The experiments were conducted at two different temperatures: 11.4°C ± 0.9° and 16.7°C ± 1.1° (Fig. 1). Each temperature regime was used for 2 tanks. Larvae were fed *Artemia salina* nauplii (Great Salt Lake Artemia Cysts, Sanders®) and commercial dry food (Vipagran Baby, Sera®) ad libitum. Dead eggs and individuals were removed at sub-daily or daily intervals.

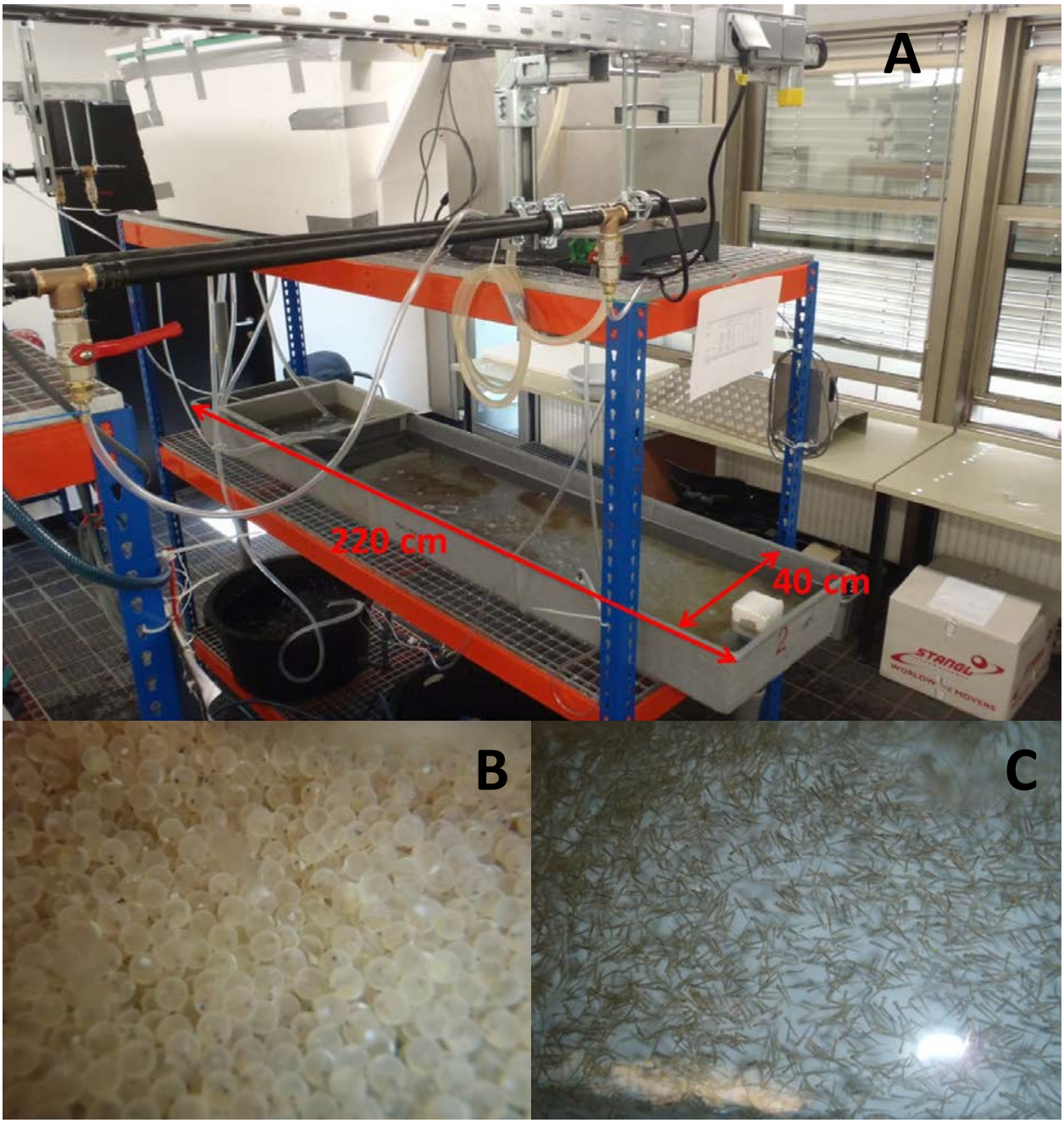

Figure 1: A) Through-flow system with temperature control, aeration system, filter (sand and gravel), and experimental through-flow tank. **B)** Eye stage eggs **C)** Larva in Stage 3 of development.

From fertilization onward, samples of 10 eggs or larvae were collected in daily intervals for 47 days from the colder tanks and for 70 days after fertilization from the warmer tanks. Before preservation in 96% alcohol, all fish were overdosed (500 mgl^{-1}) with the anesthetic tricaine methanesulfonate (MS 222).

Otolith preparation and measurements

Otoliths were prepared for further analysis by dissection after fresh weight (± 0.01 mg) was determined and standard length and total length (± 0.01 mm) were measured under a microscope (Nikon SMZ-U Zoom 1:10; Lens: ED Plan 1x) with associated visualizing software for length measurement (NIS-Elements BR 3.0).

The extracted otoliths (sagittae and lapilli) were then mounted on a slide with thermoplastic cement (Crystalbond 509 Amber). After the cement set, the mounted otoliths were polished with lapping film (grain sizes 1, 5 and 10 µm) from the sulcus side down to a thin cross-section. This was necessary for size measurements and microstructural analysis and to enhance visibility of narrow increments around the nucleus (core) of the otolith (Campana *et al.,* 1987). Otolith size was measured as minimum and maximum radius on a Zeiss AXIO Imager.M1 running ZEN 2011 software. The primordium closest to the perceived centre of the otolith was used as a starting point. The mean value of the minimum and the maximum radii of Lapilli (Figure 2A) were chosen to express otolith diameter, due to large variations of otolith morphology (Figure 2). The rostrum of the sagittae otoliths was very thin in these early stages and often broken after preparation. Accordingly, maximum radius measurements for sagittae were made not to the widest point (which is the end of the long and thin rostrum) but to the end of the more robust postrostrum on the opposite side of the otolith (Figure 2B). Otolith measurements were made at an accuracy of 0.001 µm and rounded to 0.01 µm. Microstructures were counted and analysed with magnifications ranging from 200x to 630x with immersion as required, depending on the age and size of the individual otolith. For all diameter measurements related to age estimations and growth comparisons, the Lapilli were used. Sagittae were excluded due to their rapid shape changes during early development. Asteriscii could not be used for very early stage measurements because they appear later in development than the other two (see results). Even after they first become visible, they were typically unusable for measurements of any kind because they tended to break easily and were very difficult to handle. The asterisci shown as an example in Figure 3 already shows cracks even before grinding to a depth useful for further analysis. The ring structures on asteriscii were also barely visible and irregular, making ring counts unfeasible.

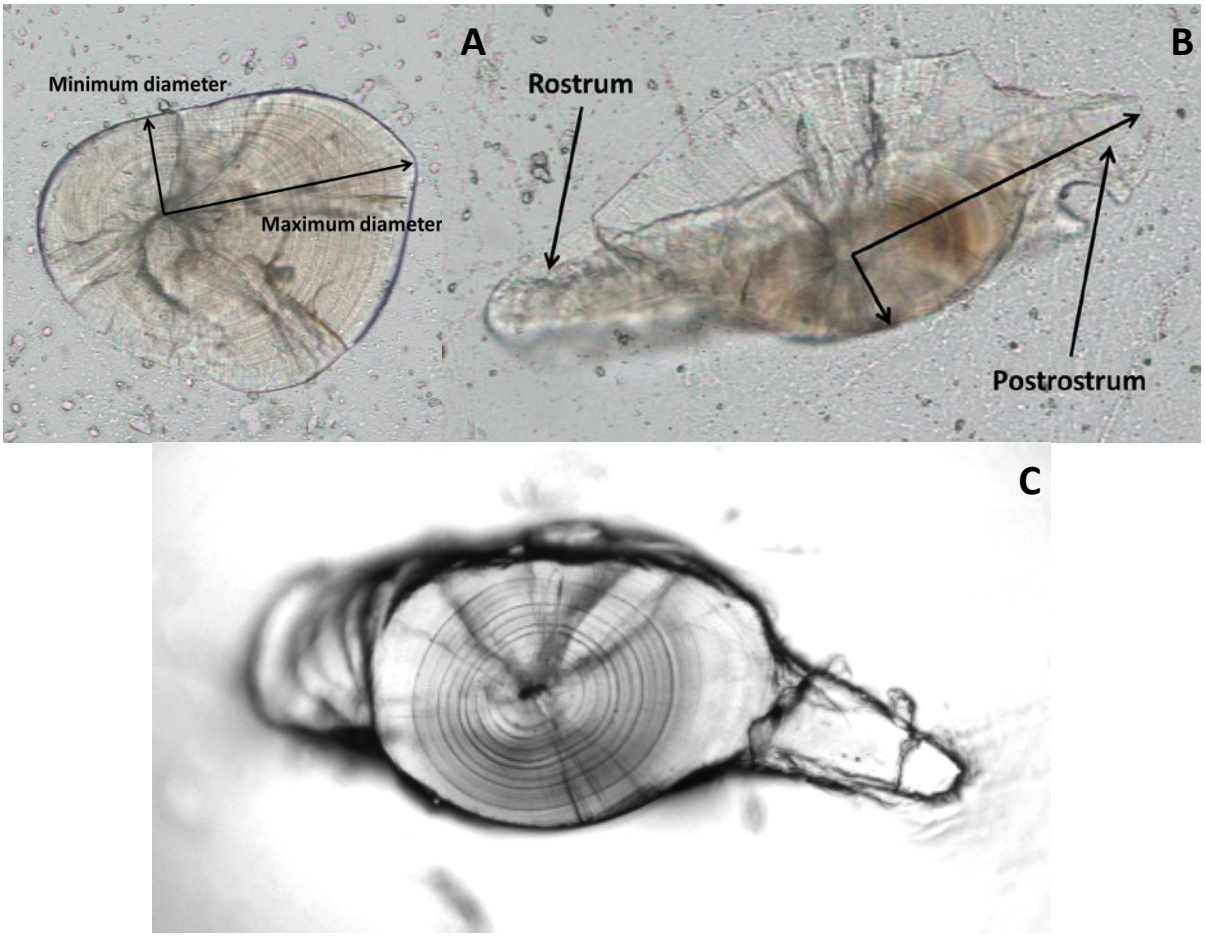

Figure 2: A and **B)** Comparison of lapillus (left) and sagittus (right) morphology from a larva reared in warmer conditions 53 days after hatch. Note different axes used for minimum and maximum diameter measurements on the lapillus, and on the rostrum and postrostrum on the sagittus **C)** 50-day-old sagittus with slightly askew positioning and broken rostrum after preparation.

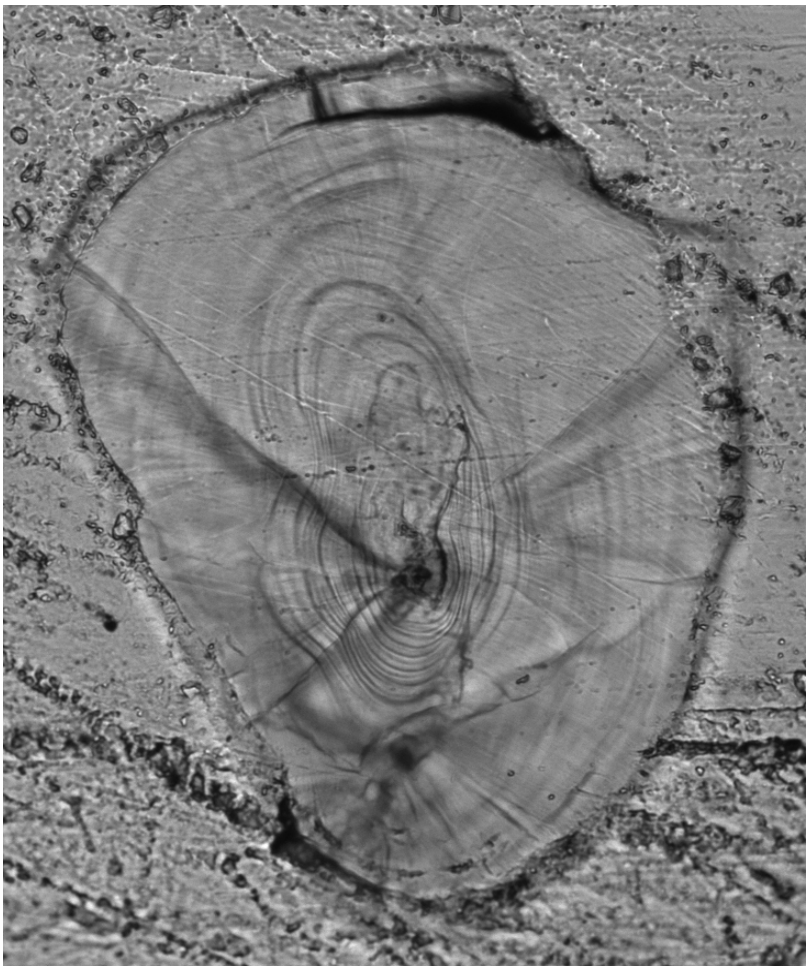

Figure 3: Asterisci taken from a nase carp larva reared at 16.7°C, 46 days after fertilization.

Examination of daily ring formation

For overall age determination of individuals, ring-counts of all four otoliths (sagittae and Lapilli) were carried out.

The age estimation by ring counts was verified with blind samples (unknown age) by the reader. The counts were then compared to the actual age after the counting procedure. The blind samples consisted of otoliths (30 + 30) from both rearing temperatures. The samples were split into two age groups (30-day periods) from both temperature regimes. Otolith samples were prepared around (± 1 day) major developmental events (i.e. at hatching, filling of swim bladder, start of the mixed feeding period), with dates in between and after at 3- to

4-day intervals. For blind age readings, samples were chosen evenly distributed through all available ages, with no special focus on major developmental events.

The first analysis of daily increments on otoliths involved counting every dark ring structure. These counts were compared to the known age, revealing errors ranging from -24 to +15 days, whereby counts made on different otoliths taken from the same larva deviated by up to 13 rings. Closer inspection of the samples regarding these errors revealed several sources (sub-daily rings, varying strength of expression, preparation errors, start of ring formation).

In order to minimize reading errors caused by sub-daily increments (Campana, 1992) and other detrimental factors, a procedure proposed by Campana and Jones (1992) was adapted and applied in this study. A confidence of readability ranging from 1 to 5 was assigned to each otolith count, with 1 being completely unreadable and 5 being easy to count. An otolith with a high confidence is defined by clearly distinguishable increments, no occurrence of artefacts or sub-daily rings recognizable by strong fluctuations of distances between rings, lighter coloration or incomplete rings. A mean count was calculated from counts of all 4 otoliths, taking into account their assigned confidence, using the formula

$$C = \frac{(C_1 * Conf_1) + \ldots (C_4 * Conf_4)}{Conf_{1+2+3+4}} \quad [1]$$

C = Weighted Mean Count, $C_{1\text{-}4}$ = individual otolith counts 1 to 4 and $Conf_{1\text{-}4}$ = Confidence of individual counts weighted from 3 to 5 (adapted from Campana and Jones 1992).

Otoliths with a confidence of 1 or 2 were discarded from further daily ring analyses, but their diameters were measured and used for the growth analysis.

The 2.5D function of the ZEN 2011 software was used to detect the difference between lighter and darker areas on the otolith surface by the simulated 3-dimensional structures (Figure 4). This feature worked best when used with a high-resolution black and white camera. In cases where contrast was the main issue, this feature completely eliminated uncertainty caused by sub-daily rings.

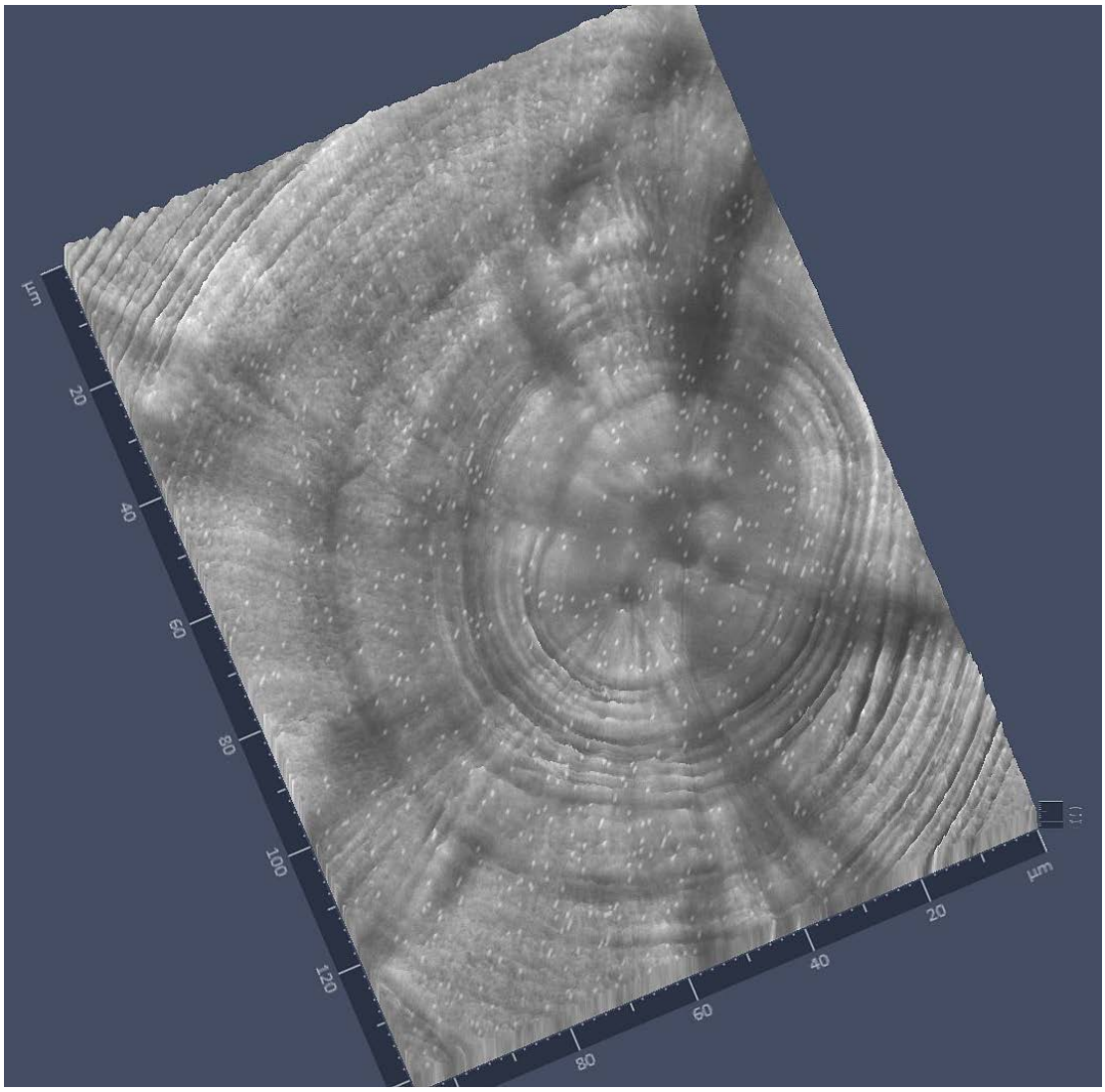

Figure 4: Simulated 3D analysis of otolith ring structures using the 2.5D function of ZEN 2011 software used for daily increment count.

Statistical analysis

For statistical tests of significance, (ANCOVA and ANOVA) SPSS© was used. Plots and linear and polynomial regressions as well as Product-Moment correlations were done using SigmaPlot©.

Results

Major developmental events

Rearing temperatures had a distinct effect on the major developmental events of larvae. There was a clear delay in development of larvae reared at 11.4°C versus 16.7°C (Figure 5, Table 1). The time spent in the egg from fertilization until hatching was twice as long for larvae in 11.4°C as it was for larvae in 16.7°C. The hatching period was also longer, lasting over 3 days (11.4°C) compared to 2 days (16.7°C). The day when 50% or more larvae had hatched was day 15 at 11.4°C and day 8 at 16.7°C. These days were used as the DoH (Day of Hatch) in all further analysis. The time between hatching and filling of the swim bladder was longer at 11.4°C (8-9 days) than at 16.7°C (5-6 days). Moreover, filling of the swim bladder occurred later in larvae from 11.4°C (day 23-24) compared to 16.7°C (day 13-14). The mixed feeding started at day 25 in 11.4°C and at day 18 in 16.7°C. Larvae at 16.7°C used up the energy reserves of the yolk sac much faster: the mixed feeding period was shorter, lasting 8 days at 11.4°C and 3 days at 16.7°C. The larvae from the colder climate used up all the yolk and reached the start of purely exogenous feeding at an age of 33 days after fertilization. The corresponding value for larvae from the warmer climate was only 19 days.

Table 1: Major developmental events in warm (16.7° ± 1.1°) and cold (11.4° ± 0.9°) rearing conditions in days after fertilization (τ, DaF).

Major developmental event	16.7°C	11.4°C
Hatching	7-8	14-16
Filling of swim bladder	13-14	23-24
Mixed feeding	18-20	25-33
Exogenous feeding	20+	33+

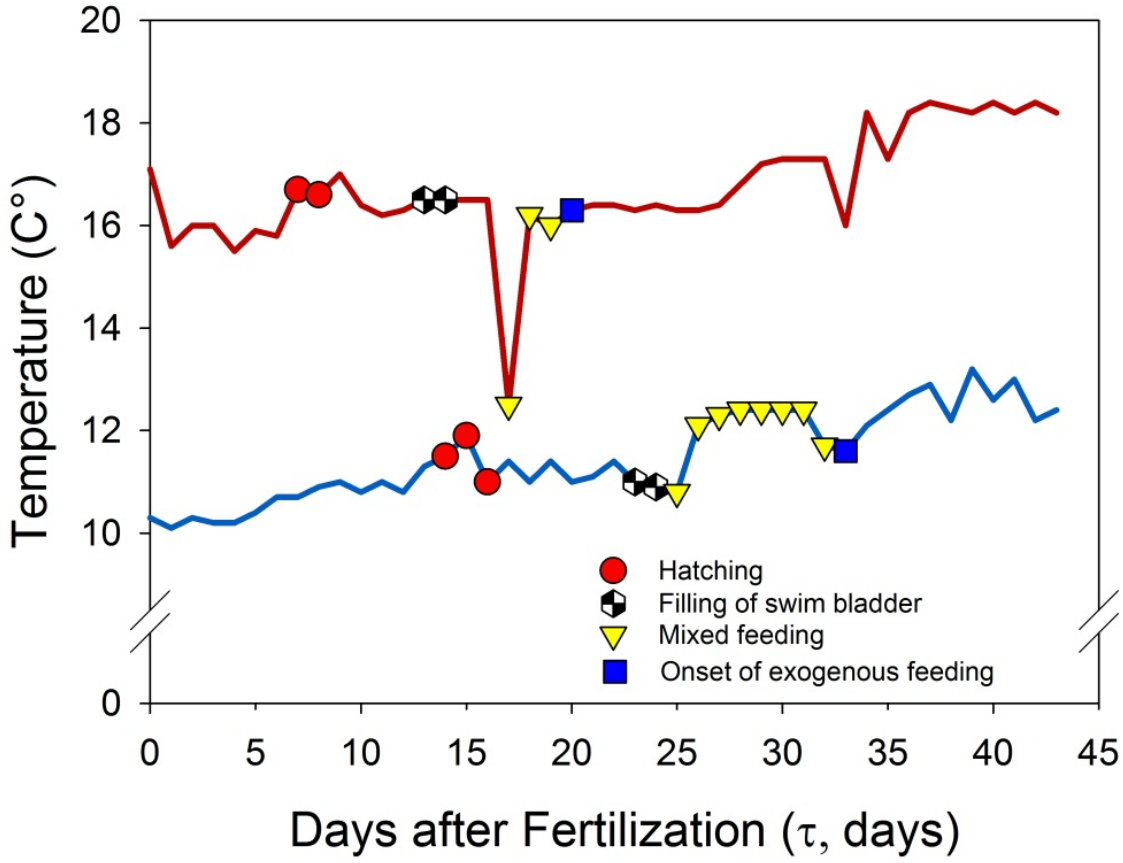

Figure 5: Temperature curve for larvae reared at two different temperature regimes. Symbols reflect the observation and duration of major developmental events.

Larval size and growth

Embryonic period

According to the classification scheme of Peňáz (1974), the embryonic period lasted 13 days after fertilization (until 5 days after hatching) at 16.7°C and 29 days after fertilization (until 14 days after hatching) at 11.4°C.

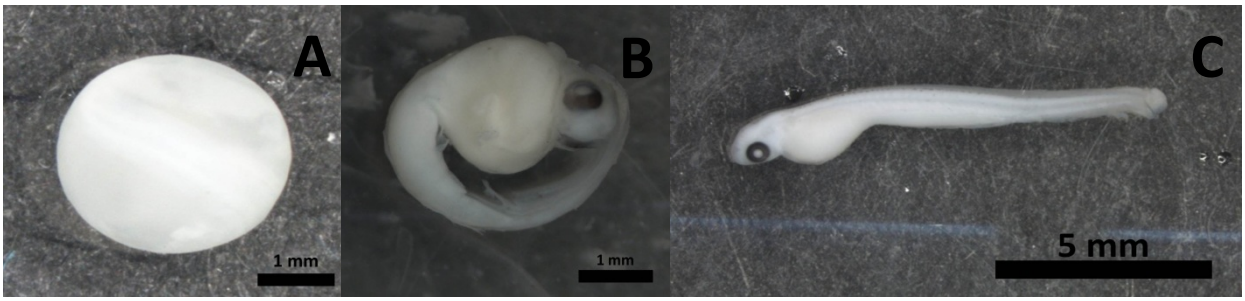

Figure 6: Image of an E7 stage embryo with (**A**) and without (**B**) egg case 1 day before hatching. **C**) Freshly hatched embryo (E8 stage (Peňáz, 1974). All reared at 16.7°C.

Larval period

Larvae reared at 16.7°C measured 10 ± 0.3 mm at hatching compared to 9.5 ± 0.9 mm at 11.4°C. At 30 DaH the larvae had grown to 15.5 ± 0.5 mm at 16.7°C and 14.3 ± 0.9 mm at 11.4°C. There is a significant difference of larval growth related to rearing temperature (ANCOVA, $F = 85.7$, $df = 143$, $p < 0.001$). The mean daily absolute growth rate (mm day^{-1}) over the first 30 DaH was 0.38 ± 0.2 mm at 16.7°C and 0.28 ± 0.05 mm per day at 11.4 °C.

From 19 DaH (16.7°C) and 31 DaH (11.4°C) onward, growth almost stagnated. This period lasted 12 days at 16.7°C, and extended throughout the remaining period (10 days) of the experiment at 11.4°C (Figure 7). At both rearing temperatures, this decline in growth rate coincided with the end of the mixed feeding period and the onset of exogenous feeding (arrow in Figure 7). In order to show these growth changes, the observed period of larval growth was split into different sections, which were compared based on several linear regressions (total length at DaF). For 11.4 °C, one regression was calculated for the period from hatching until the start of the stagnation period (DaF 31), 2 days before the onset of exogenous feeding, and one more for the remainder of the observed period. The slope of the regressions were significantly different (Table 2) and changed from b=0.21, from hatching until DaF 31 (16 days), to b=0.07 for the subsequent period (10 days). For 16.7°C the duration of the experimental period was split into 3 stages. The first stage covers the time from hatching until the onset of stagnation, 1 day before the start of exogenous feeding (11 days), with a regression slope of b=0.23. The second regression starts at DaF 19 and lasts for 12 days (b=0.02). The third regression starts at the end of the second one (DaF 31) and covers the remainder of the

plotted period with (b=0.24). A comparison of the slopes ± their 95% Confidence Intervals shows that both regressions before and after the stagnation period are very similar to each other (Table 2). The 95% Confidence Intervals overlap, therefore showing no significant difference. They both differ strongly from the slope calculated for the stagnation period (b=0.02), which indicates 11 days of almost no growth during that period (Table 2).

Table 2 Slopes (b) of regressions [TL (mm) = a + b Age (days after fertilization)] of different growth periods at two temperatures ± 95% Confidence Interval.

	Early growth	Stagnation period	After stagnation
16.7°C	0.226 ± 0.027	0.019 ± 0.025	0.236 ± 0.067
11.4°	0.213 ± 0.041	0.071 ± 0.046	n.a.

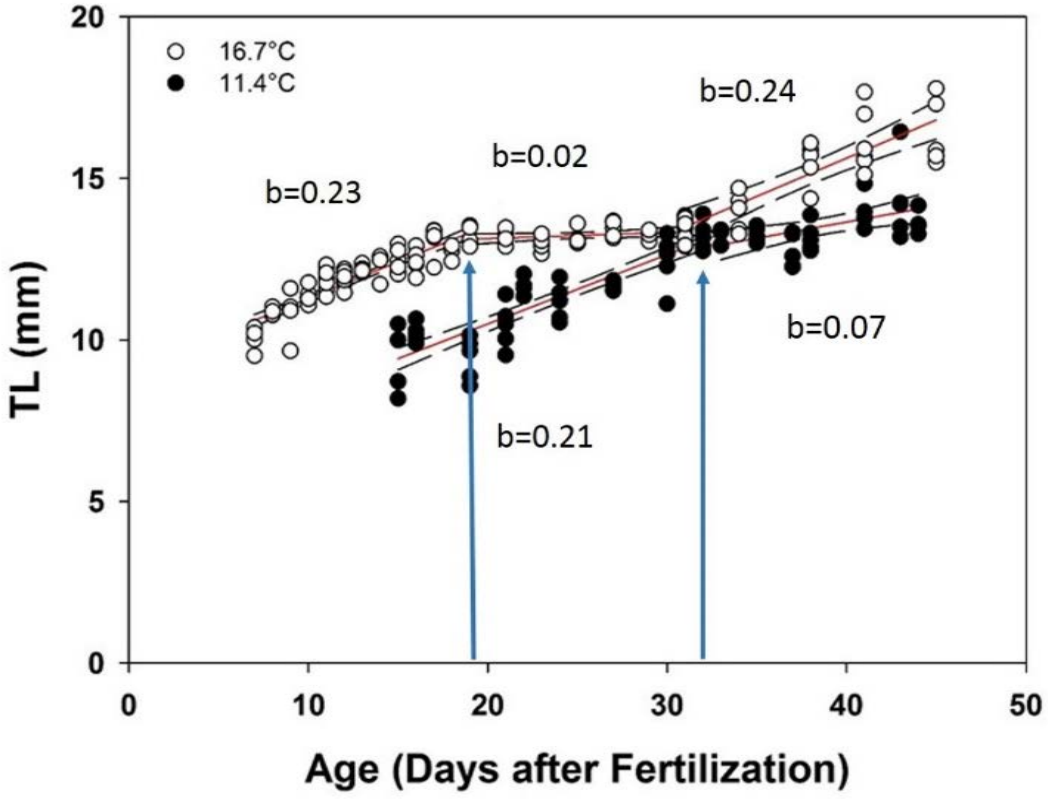

Figure 7: Growth in total length (TL in mm) of larvae at two temperature regimes. The onset of exogenous feeding after complete yolk sac absorption at both treatments is marked with an arrow (16.7°C = 19DaF; 11.4°C = 33DaF). Data were split into 3 and 2 periods by means of linear regressions for 16.7°C and for 11.4°C, respectively.

First observation of otoliths

Sagittae and Lapilli

Sagittae and Lapilli were first observed under the light microscope (10x-70x) 7 days after fertilization (= 1 day before hatching) in embryos, stages E6 and E7, with a total length of 8.15 mm (± 0.57) reared at 16.7°C. For the larvae reared in 11.4°C, the first otoliths were found in stage E7 embryos (8.07 mm) sampled at the day of hatching, 15 days after fertilization.

This constitutes the point in development at which it was first possible to observe and extract the otoliths without resorting to more complex or expensive methods. The mean diameter of Lapilli extracted from larvae reared in 11.4°C at the day of hatching (15 days after fertilization) was 53.44 µm (± 9.48); Sagittae, at the same time, had a diameter of 73.37 µm (± 15.00). For larvae reared at 16.7°C the mean diameter at day of hatch was 51.18 µm (± 3.13) for Lapilli and 72.72 µm (± 3.04) for sagittae.

Asteriscii

Asteriscii precursors were first seen 32 days after fertilization in larvae reared at 16.7° and 44 days after fertilization in larvae reared at 11.4°C (Figure 8). Irrespective of rearing temperature, the first appearance of asteriscii coincided with the physiological change from larval stage 2 to larval stage 3.

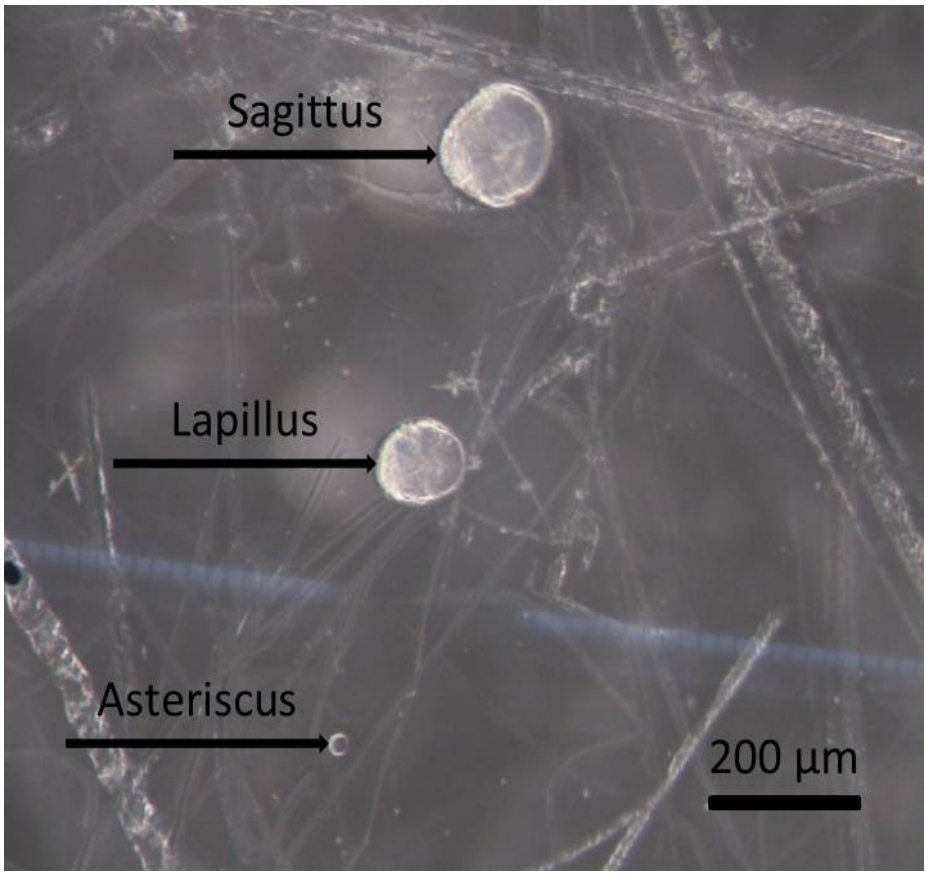

Figure 8: Size of an asteriscus at day of first observation under the light microscope (75x magnification), in comparison to sagittus and lapillus all taken from the same larvae reared at 11.4°C at an age of 44 DaF.

Otolith growth and influence of developmental events

Temperature-dependent growth of otoliths

Figure 9 shows the growth of lapilli expressed as the relationship between age and diameter at two temperatures. For this analysis, embryonic as well as larval stages of both temperatures were included (16.7°C n=51, 11.4°C n=85). At both temperatures, diameter growth was described by linear regressions (Y = a + bX). The intercepts of the regressions are given for the day of hatching and were very similar, with a = 55.41 µm at 16.7°C and a = 50.67 µm at 11.4°C. The respective slopes (b = 4.68 at 16.7°C and b = 3.63 at 11.4°C) differed significantly

(ANCOVA; F = 74.2; dF = 126; $p<0.001$), with the otoliths from the warmer temperature growing faster (Table 3).

Table 3: Intercept, slope and r^2 for linear regressions of lapilli growth in 16.7°C and 11.4°C (Figure 9).

Temperature	Intercept (a)	Slope (b)	r^2
16.7°C	**55.41 ± 3.88**	**4.68 ± 0.2**	**0.98**
11.4°C	**50.67 ± 5.44**	**3.63 ± 0.29**	**0.88**

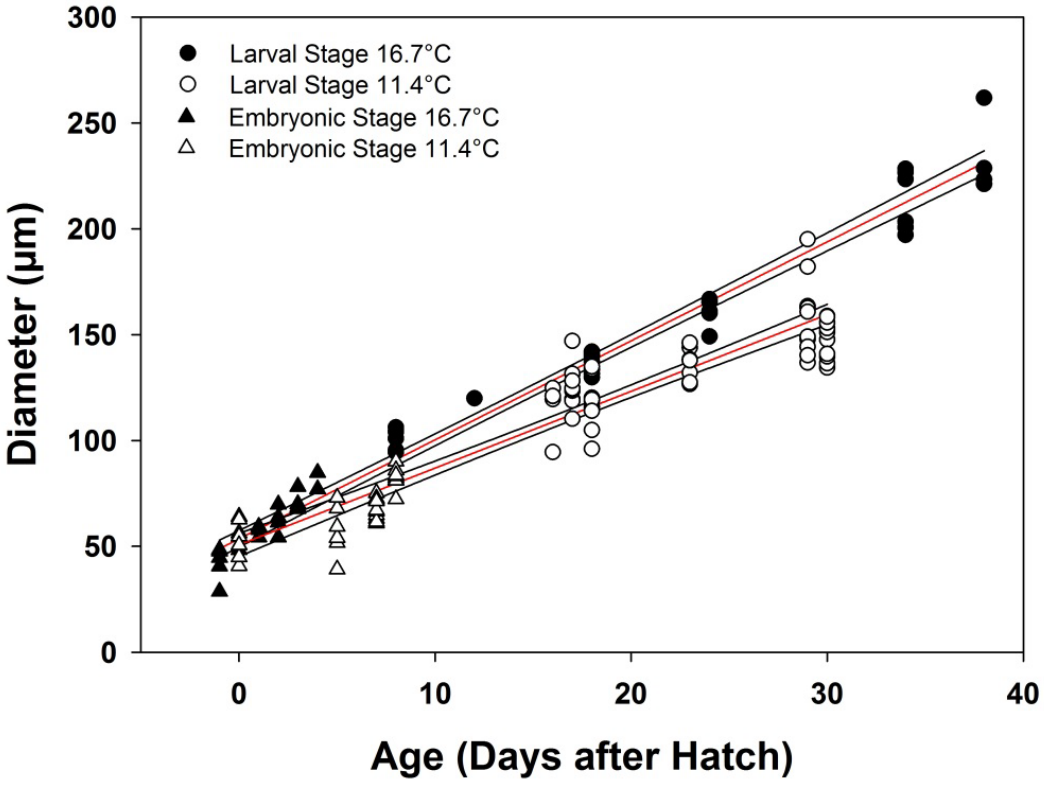

Figure 9: Relationship between age and otolith (lapilli) size at two different rearing temperatures.

The daily growth of sagittae and lapilli of individuals reared at the two different temperatures also differed by a factor of almost 2 (Table 4). For lapilli the mean growth per day over the first

30 DaH was 3.31 (± 0.74) µm at 11.4°C and 5.57 (± 1.21) µm at 16.7°C. For sagittae, mean growth over the same period was 4.3 (± 1.54) µm at 11.4°C and 8.84 (± 3.4) µm at 16.7°C.

Table 4: Average daily growth of otolith diameters and total length of larva 30 DaH in different temperature regimes. Factor = Multiplier by which growth in warm conditions was faster than in cold conditions.

Climate	Lapilli	Sagittae	Larval growth
Warm	**5.57 ± 1.21 µm**	**8.84 ± 3.4 µm**	**0.35 ± 0.13 mm**
Cold	**3.31 ± 0.74 µm**	**4.3 ± 1.54 µm**	**0.18 ± 0.07 mm**
Factor	**1.68**	**2.06**	**1.94**

Structures related to major developmental events

Hatch check

The Hatch check is a very useful structure visible as a distinct, darker and thicker band in otoliths, but its expression is species specific. For *C. nasus*, no clearly defined structure shared by a significant portion of otolith samples denoting the DoH was found.

Analysis of both sagittae and lapilli taken from larvae collected around the DoH (-1 to +3) showed that otoliths had already formed 2 rings at the time of hatching (Figure 10). A broad dark band was observed in some otoliths (Figure 10D) even before regular ring formation started. Since this structure was not as regular and clearly defined as the following rings, it was not considered in age estimations or used as a reliable marker.

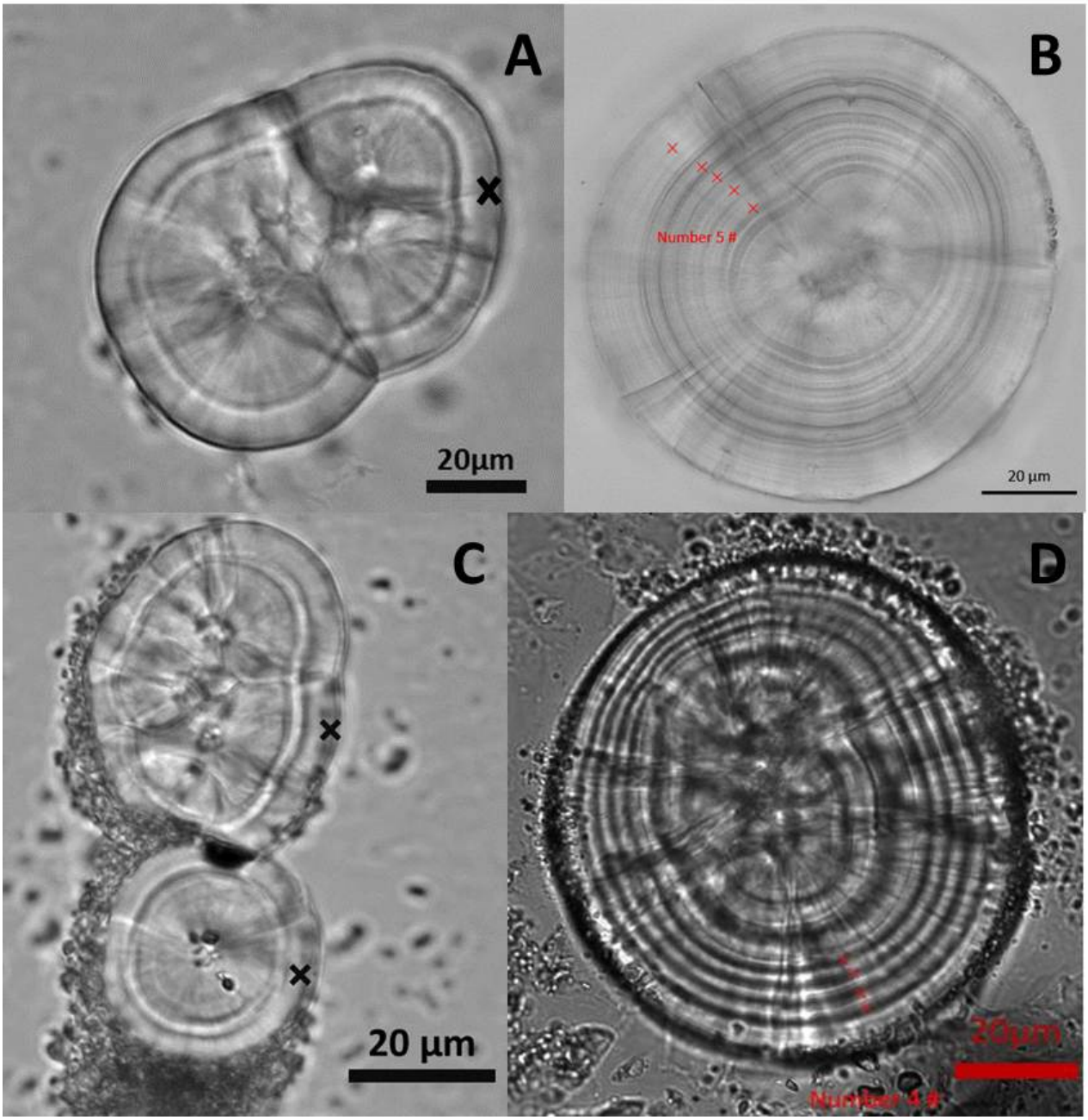

Figure 10: A) Lapillus 1 day before hatching with 1 ring visible. **B)** Sagittus 3 days after hatching with 5 rings. **C)** Sagittus (top) and lapillus (bottom) 1 day before hatch and 1 ring visible on both. **D)** Lapillus 2 days after hatch with 4 rings. Individuals reared at 16.7°C.

Mixed feeding period

The period of mixed feeding was noticeable as an area on the lapilli with broader rings in larva reared at 16.7°C (Figure 11). Distinct, darker rings at the start and at the end of this section were common, although such perceptibly darker rings are often found in varying positions on otoliths without any obvious connection to morphological events (Figure 11).

In Figure 11 the blue markings denote the area on the otolith during the mixed feeding period of this individual, showing broader rings for the duration of 4 days. This otolith was taken from a 19-day-old larva reared at 16.7°C, and the duration of enhanced growth (4 days) corresponds to the length of the mixed feeding period observed for larvae reared at this temperature, as does the time of start (8 DaH)(Figure 5, Table 1).

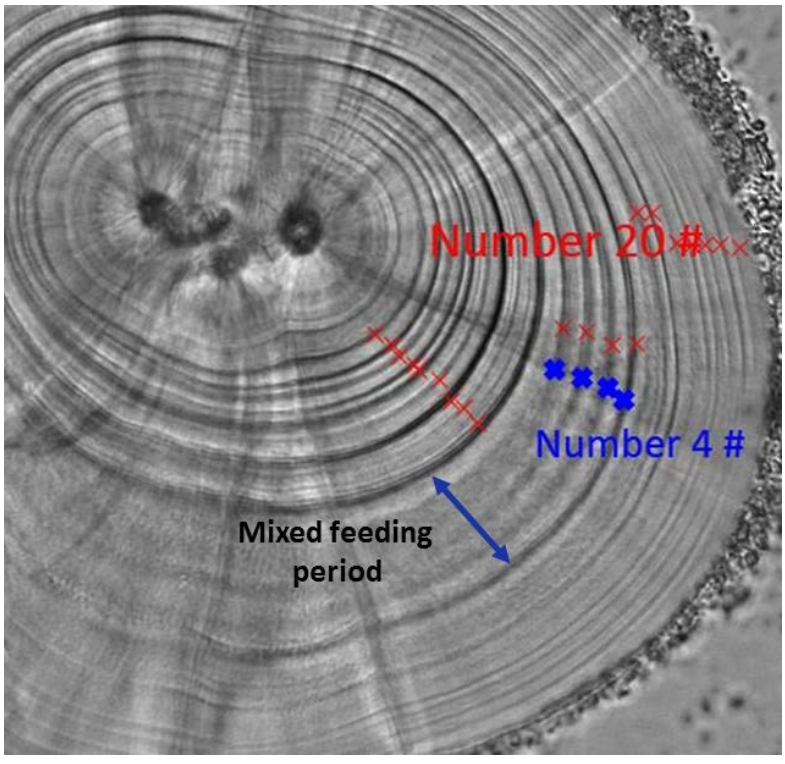

Figure 11: Lapillus (16.7°, 19 DaH) with daily ring count (red) and visibly broader rings during the mixed feeding period (blue).

Age and otolith radius

Both lapilli and sagittae otoliths were approximately the same size at hatching regardless of temperature, but showed different growth rates afterwards (Figure 12). Lapilli taken 1 day after hatching were 53.44 ± 6.86 µm in diameter at 11.4°C and 57.16 ± 1.92 µm at 16.7°C. Sagittae at the same day had a diameter of 73.37 ± 12.49 µm at 11.4°C and 86.11 ± 0.24 at 16.7°C.

The size/diameter of lapilli from individuals from both rearing temperatures increased significantly with age. This relationship could be described by a linear model, with the otoliths from the colder climate growing significantly slower (ANCOVA for effect of temperature on diameter; F = 74.2; dF = 124; $p<0.001$). This difference is clearly indicated by significantly different slopes of the regressions (16.7°C b = 4.68 ± 0.21; 11.4°C b = 3.6 ± 0.29). The growth of sagittae showed a curvilinear pattern (Figure 12B).

In the warmer climate the mean growth per day of lapilli over a period of 30 days after hatch was 5.88 ± 1.78 µm. For sagittae over the same period the value was 10.45 ± 3.36 µm. For larvae reared in the colder temperature, the mean growth per day over a period of 30 days was 3.31 ± 0.74 µm for lapilli and 4.3 ± 1.54 µm for sagittae (Table 4).

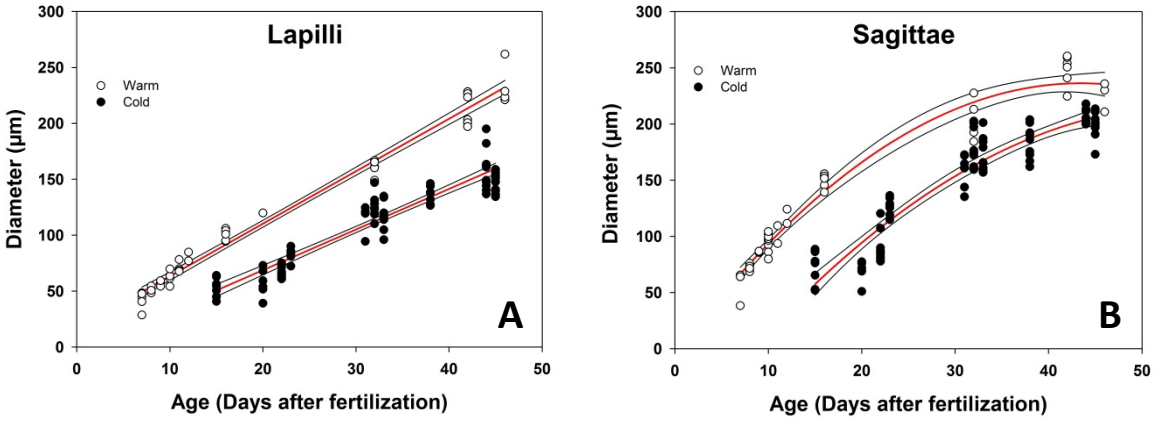

Figure 12: Comparison of size and growth of **A)** lapilli and **B)** sagittae at two different temperature regimes (warm = 16.7°C; cold =11.4°C).

Otolith growth

Irrespective of rearing temperature, the size of fish expressed as total length (in mm), otolith diameter (lapillus, µm) and the estimated age from ring counts correlated highly significantly with age in days after hatch (DaH)(Table 5). The highest percentage of variability (99.5%) was explained by the age estimation of ring counts, followed by otolith diameter (87.5%) and fish size (71.8%).

Table 5: Pearson product-moment correlations coefficient of determination from linear regressions comparing age to three different variables. Regressions: Tl (TL = 10.76 + 0.14*DaH); Lapillus diameter (Diameter = 37.06 + 4.72*DaH); weighted count (Ring Count = -0.03 + 0.99*DaH)

Age compared to	r^2	P	n
Total length (mm)	0.718	<0.001	205
Lapillus diameter (µm)	0.875	<0.001	135
Ring count (weighted)	0.995	<0.001	56

A relationship ($r^2 = 0.94$; $p<0.001$; $n = 135$) between lapilli diameter and total length was highly significant (Figure 13) for the combined data from both temperatures.

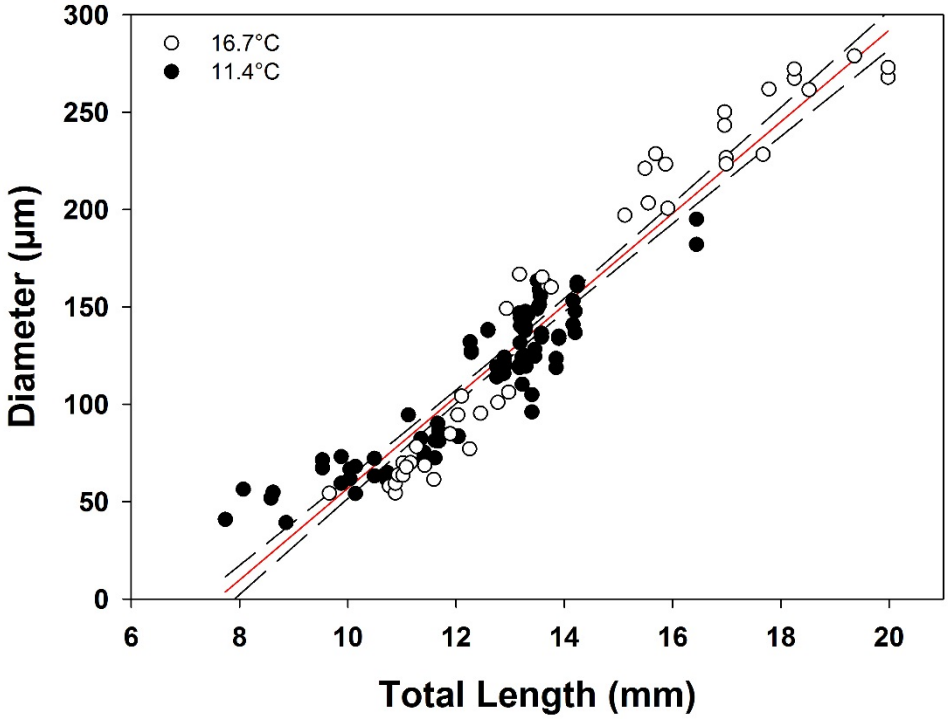

Figure 13: Relationship between lapilli diameters from both 16.7°C and 11.4°C (figure 12A) compared to the total length of the larvae they were taken from. Linear regression (r^2 = 0.91) plotted with confidence intervals (95%). Regression (Y = -178.59 + 23.54*X).

Simulated age estimation of larva using otolith diameters

In order to simulate estimating the age of wild-caught larvae using lapilli diameters, a linear growth model was fitted from diameter measurements of known-age larvae from both temperatures. For this purpose the data in Figure 13 were used, but total length was compared to known age (DaH). The resulting linear regression model of $Diameter = 49.93 + 4.07 * Age_{known}$ was adapted to give an estimated age from a known Diameter $Age_{estimated} = \frac{Diameter - 49.93}{4.07}$. This formula was then used to calculate an estimated age from lapilli diameters from both temperatures, and the results were plotted against the actual age in DaH (Figure 14). The age estimations showed individual errors ranging from – 9.2 days to + 14.0 days and a mean error of 3.1 ± 2.5 days. A linear model fitted to the estimated ages showed an r^2 of 0.88 and a slope very close to 1 (1.0018).

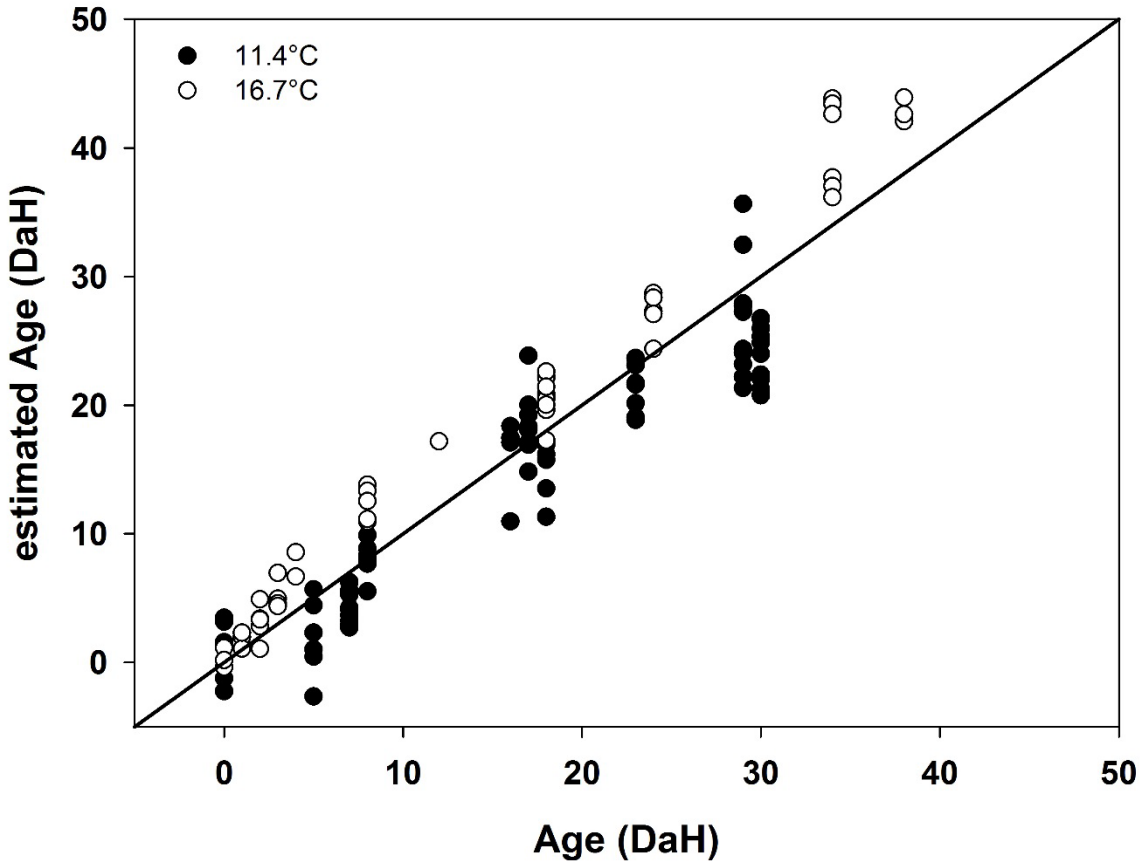

Figure 14: Estimated age of larvae using lapilli diameter measurements of from both temperatures compared to actual age. Line representing 1:1 axis (actual age).

Daily ring deposition

In order to analyse a diurnal cycle of substance aggregation in otoliths of larvae of nase carp, otoliths (n = 10) marked with Alizarin at a known time were studied. These observations showed that the mark was incorporated in the lighter areas of the daily ring in the otolith, which consists mainly of $CaCO_3$ (Figure 15). This also means that the darker rings on the otolith, consisting mostly of matrix protein, must be incorporated at another time, probably during the night. Moreover, the 4-day interval between treatments was reflected by the number of dark or light rings, verifying deposition of 1 light and 1 dark ring per day.

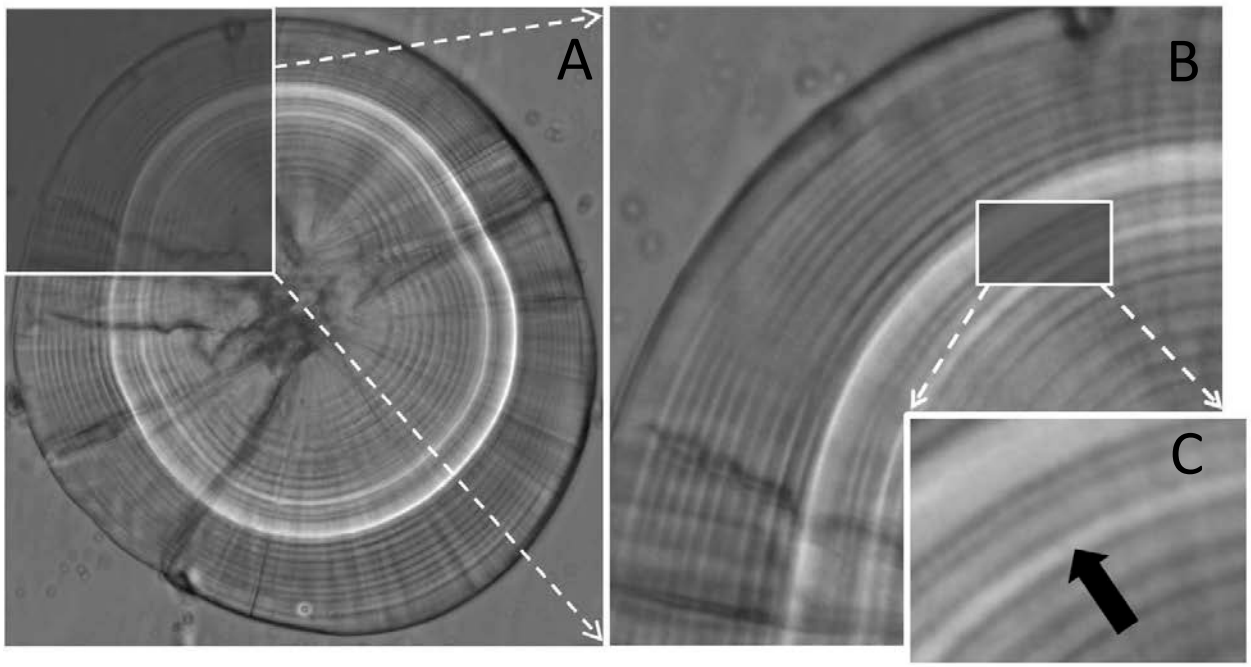

Figure 15: Otolith from larval stage 5 nase carp with two fluorescent markings applied at a known time during the day, at an interval of 4 days (**A**, **B**). The arrow points to one of the two markings, visible between two dark rings, thus incorporated during $CaCO_3$ accretion (**C**).

In addition to a diurnal cycle of light and dark patterns, additional sub-daily increments reflect masking, fluctuating environmental variables such as temperature, and feeding (Campana, 1992) (Figure 16). Detailed follow-up examinations showed that sub-daily increments were by far the biggest factor in, for some cases very substantial, counting errors – especially in otoliths from very young larvae (<30 days) ranging from -24 to +15 days.

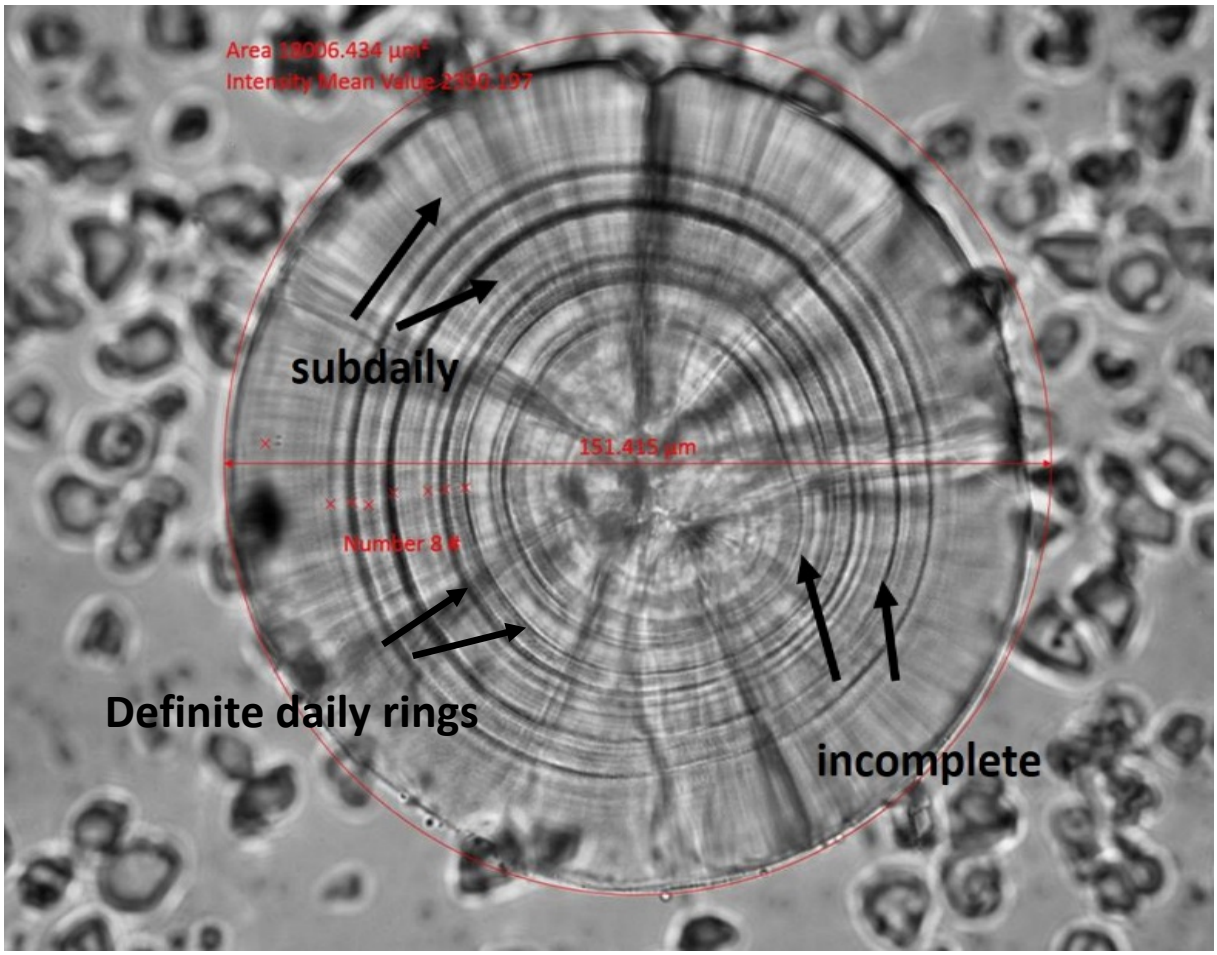

Figure 16: Sagittus 9 days after hatching with incomplete and sub-daily increments.

Daily increment counts

First test of procedure

In a first test, daily increments along an axis chosen based on the quality of visibility, were counted from otoliths of 26 random samples without any further regard to preparation quality, starting age of ring formation or continuous ring formation. The individual errors in these counts from larvae aged 1 to 60 DaH ranged from an underestimation of 24 days to an overestimation of 15 days (Figure 18A).

Counts made on different otoliths taken from the same larvae deviated by up to 13 daily increments. A linear regression model comparing these counts to actual age revealed an r^2 of

0.69. In Figure 18A the margin of error in these counts is compared to a 1:1 axis representing the actual age of the larvae.

In order to increase the precision of the age estimation, the first correction involved subtracting 2 days due to the observation of 2 formed rings at DoH (Figure 10). Furthermore, the existence of sub-daily rings of differing strength had to be taken into account. This meant excluding those light-dark structures along the counting axis that did not form a continuous ring or that appeared in very random intervals lacking distinct, evenly spaced light and opaque zones (Figure 16). Finally, the strict adherence to a single straight counting axis was deemed not only unnecessary but detrimental to the overall accuracy of daily ring counts. The rings were counted from the center, following no strict axis or path but jumping from the respective area of best visibility of each ring to the area of best visibility of the next. Visibility was defined by the strength of contrast between light and dark areas. The appearance of daily depositions of matrix proteins, visible as dark bands, ranged from almost black to a very light grey. The higher the contrast between light and dark depositions, the better defined the daily ring. This makes some rings definite, observable daily depositions, contrary to low-contrast, light grey depositions. This discrepancy leaves certain inclusion of lower contrast depositions into a count open to interpretation of the reader.

Rings were counted on blind samples (unknown age) and assigned a confidence value ranging from 1 to 5, subjectively defined by the reader, with 1 representing lowest confidence and 5 highest confidence in the accuracy of the count. Preparation quality, visibility of individual rings and evenness of space between ring structures were all taken into account to make this classification scheme as objective as possible. An analysis of the assigned confidences showed that the deviation of the actual ring counts clearly decreased with increasing assigned confidence (Figure 17A). A high frequency of confidence values 3 and 4 correlates with an increase in accuracy. Confidence values 1 and 5 were scarce compared to the others (Figure 17B), but in all cases seemed justified. Confidence value 2 counts were very accurate in some cases but spread over an interval ranging from plus 4 days compared to actual age to an underestimation of 8 days. This inaccuracy at value 2 led to their exclusion from all further analysis together with value 1 counts, which by definition were classified as “unreadable”.

After discarding counts with assigned confidence values 1 and 2, 54% of all potentially usable otoliths featuring an adequate quality of readability remained for further analyses (n=101).

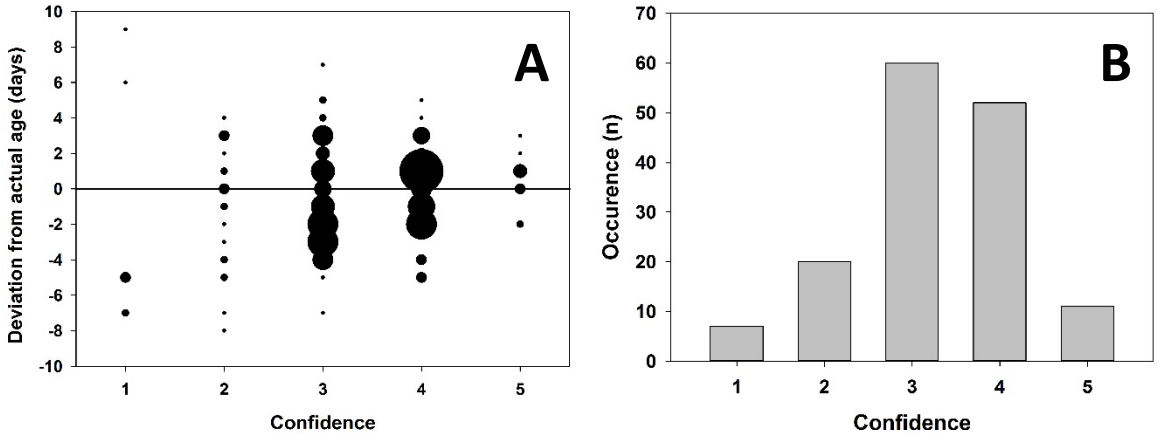

Figure 17: A) Assigned confidence and error of individual counts of otoliths, with size of bubble representing frequency of occurrence (n=150); **B)** Frequency of assigned confidences (n=150)

After refining the counting procedure and including a weighted mean (Formula 1), as proposed by Campana and Jones (1992), the r^2 of a linear model fitted to the age estimations increased from 0.69 to 0.98. The accuracy of age estimation was considerably improved and ranged from a maximum value of ± 5 days (Figure 18B). Ring formation on a daily basis could be verified with an accuracy of 1.8 ± 2.2 days of actual age for a mix of samples from both temperatures over the whole sampling period of 47 DaF at 11.4°C and 70 DaF at 16.7°C.

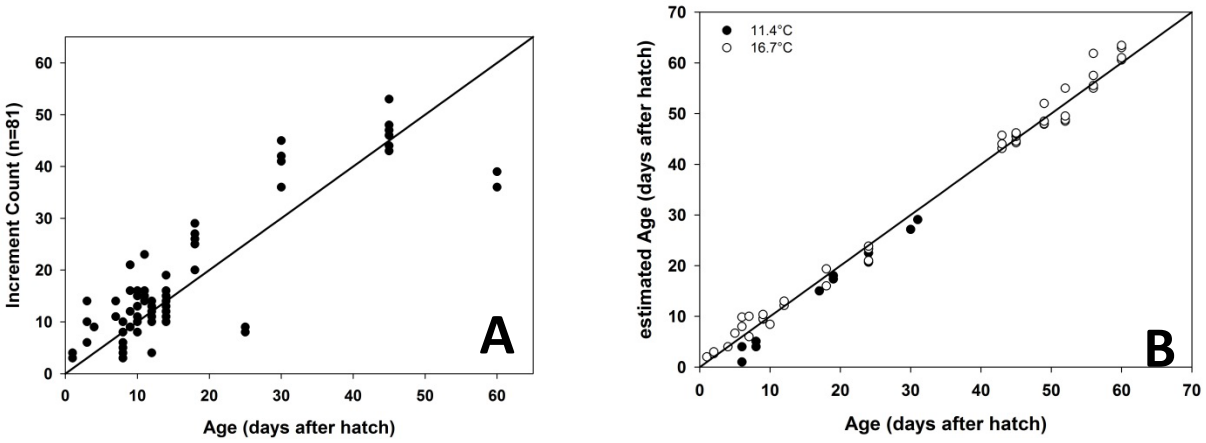

Figure 18: A) Relation between actual age and counts of every dark ring structure of the otolith. Line represents 1:1 relationship. **B)** Actual age after hatching of larvae compared to estimated age from ring counts using the method from Campana (1992). Lines represent1:1 relationship.

Discussion

Developmental events

Distinct structures, generally larger darker rings, related to specific developmental events have been reported for many fish species. These structures, termed “checks”, have been interpreted as markers of life history events such as hatching, metamorphosis, environmental stress, or habitat transitions (Campana, 1984; Neilson *et al.*, 1985; Karakiri *et al.*, 1989; Gartner, 1991; Geffen, 1996; Modin *et al.*, 1996, Morales-Nin, 2000). A check formed at the day of hatch has been reported for Pacific cod *Gadus macrocephalus* (Narimatsu *et al.,* 2007), bony flying fish *Hirundichthys oxycephalus* (Chang *et al.,* 2012), fat greenling *Hexagrammos otakii* (Joh *et al.,* 2008) and black-spot tuskfish *Choerodon schoenleinii* (Yamada *et al.,* 2009). The Nile tilapia *Oreochromis niloticus* (Zhang and Runham, 1992) forms a check 1 day after hatching. Japanese anchovy *Engraulis japonicas* (Tsuji and Aoyama *et al.,* 1984) and Japanese pilchard *Sardinops melanostictus* (Hayashi *et al.,* 1989) both form a distinct check at first feeding, as does the cresthead flounder *Pseudopleuronectes schrenki*, which forms a check 6 days post hatch, the time of both complete yolk-sac absorption and first feeding (Joh *et al.,* 2014). Changes in feeding behavior, coupled with the respective morphological changes, seem to be events in the early life of larvae that are often reflected by visible structures in otoliths. For brown sole *Pseudopleuronectes herzensteini* (Joh *et al.,* 2011), greenback flounder *Rhombosolea tapirina* and longsnout flounder *Ammotretis rostratus* (Jenkins, 1987), a check is formed during transition from endogenous to exogenous nutrition. In the case of *C. nasus*, no distinct structure relating to hatching or any other event was observed. Darker, more prominent rings were present on most of the otoliths, but they varied in position and could not be related to a specific event.

The period of mixed feeding was visible as a zone with broader increments on lapilli of larvae reared at the warmer temperature. The enhanced growth in lapilli from those larvae was recognizable as a distinct event without resorting to measuring and comparing specific increment widths. For larvae reared at 11.4°C, no enhanced growth during that period was evident. Measurements of individual increments would be needed here, i.e. comparing growth during mixed feeding with endogenous and exogenous periods. The overall slower

growth, also reflected by otoliths, clearly decreases the visibility of any effect of enhanced growth during a specific period. Additionally, the mixed feeding period for 11.4°C-reared larvae was twice as long, spreading any positive effect on growth over a longer period and therefore masking it further. These findings agree with earlier observations in the field and laboratory, which have shown that increment width may change in response to temperature and diet, but that the period of increment deposition remains daily (Gauldie and Radtke, 1990). Note, however, that information on enhanced otolith growth specifically during mixed feeding has never been reported before for other species. An interesting result was the clear slowdown in larval growth (length) for a period of 10+ days after the mixed feeding period (Figure 7). This was reflected by smaller increment widths during that period, making a small increase in growth directly before that period much more evident.

Larval size and growth

Embryonic period

During the embryonic period the main food source available to embryos is the yolk (Kamler, 1992). This provides a fixed amount of energy to every individual. Any difference in development speed can be attributed solely to temperature-dependent metabolic rates of the individual organisms. Temperature has been demonstrated to affect every aspect of fish early development: hatching, emergence and initial feeding times (Alderdice and Velsen, 1978; Beacham and Murray, 1990; Blaxter, 1992; Ojanguren, 1999). In the present case, changing the temperature regime in the tanks from 11.4°C to 16.7°C shortened the embryonic period from 29 DaF to 13 DaF. This physiological response reveals the controlling effect of temperature on metabolic processes through thermal dependence on enzymatic activity (Brett, 1970; Rombough, 1988; Blaxter, 1992; Kamler et al., 1998).

Larval period

Within a species-specific range, the effect of higher temperature is faster growth (Ojanguren & Brana, 2003; Cossins & Bowler, 1987; Blaxter, 1988; Atkinson, 1996). Both of the

temperatures used in the present study were in a range that enabled larval development without any drastic increase in mortality (Keckeis et al., 2001). The faster growth in warmer temperature was distinct, and a non-linearity was evident at both temperatures. The observed non-linearity in the present case did not reflect a slowing down of growth with age, but rather a notable slowdown for a period of time after the end of the mixed feeding period. The larvae reared at 16.7°C showed a definite end to this period of stagnation after 11 days. Thereafter, growth continued at the same pace as earlier (see regression slopes in Figure 7). Larvae reared at 11.4°C also grew slower during the same time in development (end of mixed feeding), as did those reared at 16.7°C, but the decrease was less pronounced (Figure 7). At the 11.4°C experiment, samples were available only for 10 more days after stagnation began. In these 10 days, growth did not accelerate again, as it did for larvae from 16.7°C after 11 days. Nonetheless, one interpretation is that an acceleration similar to that recorded in the larvae from the warmer habitat would have been observed if the sampling period was longer. For both temperatures, the onset of the period of retarded growth coincided with the switch to purely exogenous feeding. A similar period of slow growth at the same stage of development has been observed in *Sander lucioperca* (Löffler *et al.,* 2008) and *Zingel streber* (Kovác 2000).

Start of exogenous feeding

The onset of exogenous feeding is a crucial time in developing fish larvae (Yufera and Darias, 2007). Here, larvae undergo massive morphological changes, enabling them to actively seek out (eyes and chemosensory organs), catch (mouth, fins and muscles) and digest (digestive system) external food sources. Moreover, cutaneous respiration is replaced by gill respiration and the respiration rates increase exponentially (Kamler *et al.,* 1998). All these internal morphological changes are a major drain on energy resources, diverting the focus away from physical growth. Yufera and Darias (2007), for example, propose to consider the onset of exogenous feeding as encompassing the point at which ingestion is possible up to the moment when larval growth begins.

First observation of otoliths

Sagittae and Lapilli

Both sagittae and lapilli were first found two days before hatching. An effort was made to compare the otolith growth data available for *C. nasus* with early stage growth analyses of *Danio rerio*, an extensively studied cyprinid and well-known "model organism" for early stage larval anatomy and development. Otoliths are one of the very first calcified structures to appear in most teleosts (Campana, 1985), and *D. rerio* show a first growth spurt of otolith precursors 19 to 24 h after fertilization (Wu *et al.*, 2011; Haddon and Lewis, 1996). In order to estimate the emergence of otoliths in *C. nasus*, the average growth rate after hatching was used to back-calculate a point of emergence. Hypothesizing a similar otolith growth speed before and shortly after hatch, combined with the fact that *D. rerio* is a model organism for cyprinid fish and their early development, it is reasonable to assume that the early stage otolith developments documented in *D. rerio* translate well to *C. nasus*.

Asteriscii

In addition to the late appearance of asterisci compared to the other two pairs of otoliths, they have a different crystalline structure in the $CaCO_3$ parts. In all cyprinids, asteriscii are composed entirely of vaterite instead of aragonite (Escot & Granado-Lorencio, 1998; Lenaz *et al.*, 2006; Gao *et al.*, 2009; Li *et al.*, 2009; Yang *et al.*, 2009; MacDonald *et al.*, 2012). The late appearance suggests that asteriscii are not immediately essential to the larvae but fulfil more of a complementary role.

Otoliths lie over patches of sensory hair cells, where they provide an inertial mass load for sensing gravity and linear acceleration. In fish they are also used for hearing (Popper and Lu, 2000; Abbas and Whitfield, 2010; Stooke-Vaughan *et al.*, 2012). An exact definition of the specific, individual role filled by Asterisci, or the other two otolith pairs of *Chondrostoma nasus*, cannot be given. The specific roles of the individual otoliths remain unclear (Popper and Lu, 2000). Evidence suggests that otoliths have different functions in different species and may, in many species, have both auditory and vestibular roles (Platt and Popper, 1981; Platt,

1983; Popper and Fay, 1993; Popper and Platt, 1993). An indication as to the possible function of asteriscii might be their time of emergence, which coincides with a shift from larval stage 2 to 3. At that point, *C. nasus* larvae already aggregate in shoals, show rheophilic behavior and the anterior chamber of the swim bladder starts to fill with gas. These changes greatly enhance swimming ability and, with that, the need for good spatial awareness and predator detection. One interpretation is that asteriscii enhance or refine one or both of these aspects. The huge diversity in teleost fish (30,000+ species) complicates comparing any findings concerning otolith form and function between species. The anatomical variation in the ears across fish species is probably greater than in any (perhaps all) other vertebrate groups (Retzius, 1881; Popper and Fay, 2011). Evidence for this huge diversity in form and function is shown by the variation in the bandwidth of hearing, which exceeds that of any other vertebrate group: some species hear only up to 100 or 200 Hz, others, all in the genus *Alosa*, that can hear to well over 180 kHz (Plachta and Popper, 2003; Mann *et al.* 2001). One conclusion is that, for aging purposes as well as species identification, the other two pairs of otoliths (sagittae, lapilli) are preferable to asteriscii. For aging purposes on the scale of days of *C. nasus*, the otolith of choice would be the lapillus. For species identification, the sagittae serve well because they show the largest morphological variability of the three otolith pairs and, in adult fish, are the biggest and easiest to handle. The biggest problem in working with asteriscii in these early stages is the vaterite structure of the $CaCO_3$: compared to the aragonite composition of the other two, it is very brittle and therefore extremely difficult to handle. Moreover, they appear later in development and the daily rings are expressed very irregularly and with low contrast (Figure 3).

First ring formation

On both lapilli and sagittae, two daily increments were already visible at the time of hatching. This shows that the circadian rhythm of matter deposition on otoliths is already established and functional at a very early stage in *Chondrostoma nasus*. In general, the circadian rhythm responsible for the daily rings on otoliths is regulated by the pineal gland, which establishes a biological clock using specific photoreceptors generally termed “Third Eye” (Kulczykowska *et al.* 2010). This rhythm is entrained very early in development and is applied to many

physiological functions. The exact time its first use to regulate the deposition of $CaCO_3$ and matrix proteins in fish otoliths, as well as any ties to other developmental events, are apparently highly species specific. The fact that two daily rings are already established at hatching is visible only in *Chondrostoma nasus*; for other species the formation date of the first daily increment might differ and, in some, it will be coupled to developmental events. The Californian Anchovy (*Engraulis mordax*), for example, produces a first daily increment 4 to 5 days after hatching, coinciding with completion of yolk-sac absorption (Brothers *et al.*, 1976). This species-specific start of daily ring formation makes verification of first ring formation essential for every species before starting to work on age-related counting procedures based on daily ring deposition**.**

Temperature dependency of otolith growth

Fish, being cold stenotherm organisms, show a strong temperature dependency in all their physiological processes. This is reflected in the growth speed of both larvae and otoliths as well as in rate of development from time of fertilization. Otolith diameters reflect the size of the larvae they were taken from (Figure 13), which is influenced by habitat temperature and larval age (Figure 9). This requires daily ring counts for age estimations if no exact data are available regarding ambient temperature in conjunction with a calibrated growth curve. The two different temperature regimes used here differ by approximately 5 degrees (11.4° ± 0.9° and 16.7° ± 1.1°), but in the first 30 DaH, average larval growth as well as otolith growth in the warmer climate is almost twice that of the colder climate (Table 3).

This faster otolith growth in warmer temperatures is also visible in otoliths of adult fish from temperate zones as annual rings, where times of lower temperature form a darker ring due to slower growth (Casselman 1987). One use for the temperature-dependent otolith sizes at the same age would be to estimate the temperature in the nursery habitat by comparing estimated age (from counts) to diameter measurements. The strong temperature dependency of physiological growth, including otoliths, is a recurring theme in all age estimations in fish using morphological parameters. A simulated age estimation based on otoliths from the two

temperature regimes showed the resulting inaccuracy, with individual errors ranging from -9.23 to + 14.01 days for samples from DoH to 38 DaH. Since only larva from two different temperatures were used here, it is safe to assume that the errors would be even greater if the temperature were an unknown somewhere in the survivable range for *C. nasus*. In the Danube east of Vienna, a natural habitat of the *C. nasus*, the temperature during the larval period ranged from 9.2°C to 17.1°C with a mean of 12.81°C ± 1.73°C. This range is quite well covered by the two temperatures, 11.4°C and 16.7°C, used.

Accuracy of age estimations

Age estimations based on daily ring counts were the most accurate method to estimate larval age (Table 4). A key element in increasing the accuracy of counts, beyond the methodological improvements, was to establish the date of first increment formation. For *C. nasus* the two increments already established at the time of hatching considerably influenced the counting accuracy. For other species this bias can be much greater and must be kept in mind for all age readings done on otoliths.

Circadian rhythm of ring formation

The otoliths marked with alizarin red (Figure 15) were used to compare the present results with results from other studies, i.e. on *Salmo gairdneri* (Mugiya 1987). Ca is incorporated in otoliths as $CaCO_3$ – visible as white regions under a light microscope – and glutamic acid as a part of the otolin matrix protein complex – visible as dark bands between the broader $CaCO_3$ regions. Mugiya (1987) showed that the pace of otolith calcification is almost antiphasal to the pace of matrix deposition on otoliths, with a peak at 1600 h for calcification. Using the fluorescence markings made at noon did not enable this level of precision concerning deposition rates, but it became clear that, at the time of alizarin incorporation, $CaCO_3$ was aggregated. Nevertheless, it is highly probable that, given the similar light-dark phases in the habitat, the deposition rates over the course of a day are similar in *S. gairdnerii* and *C. nasus*.

Daily increment counts

Methodology

The procedure used to establish age data was significantly altered following Campana (1992) after a first run, which only used a simple count of daily rings along a fixed axis. This was necessary because the time of first ring formation distorted accuracy and because the different visibilities of rings on otoliths or sub-daily rings influenced the precision of counts. The methodological alterations markedly increased the accuracy of counts; without these alterations, daily ring counts were very inaccurate given the effort needed. After this refinement, the daily ring counts were the most accurate method and showed no temperature bias.

Comparison of methods

Measuring larval length, for use in an age-length key, is by far the fastest way to estimate age, but requires knowledge of species and a window of habitat temperature as narrow as possible. Moreover, the age-length key (Coggins 2013) has to be established first. This is preferably done under laboratory conditions. Otolith diameters provide better accuracy than an age-length key (Table 4), but otolith size is also strongly temperature dependent (Figure 9). The trade-off for the increased aging accuracy of otolith diameters versus simple length measurements is the time necessary to gather the data. Daily ring counts showed the best accuracy (Table 4) and there was no temperature dependency. This was also the most labor-intensive method.

Overall, the appropriate method of age estimation heavily depends on the respective goals and resources. For most cases in which wild caught larvae are to be aged, a mix of methods will be the best solution. As noted above, one factor strongly involved in the accuracy of aging larvae is the amount of time invested. Counting daily rings becomes unfeasible with bigger sample sizes due to the many steps involved. A good tradeoff between accuracy and effort

can be achieved if daily ring counts are not used to age all larvae but to establish a linear model ($Y = a + bX$), comparing estimated age based on ring counts to the respective fish length or otolith diameter. This essentially provides an Age-Length (Coggins 2013) or Age-Diameter key. Using the weighted mean of daily ring counts of larvae from an unknown temperature as X (Age in days) in a linear regression model enables inserting the corresponding otolith diameter or total length data. This yields an intercept (a) and slope (b) for the model. After establishing these parameters, the resulting model can be used to calculate Y (estimated age) using the respective parameters, without a bias towards temperature. This bias would in this case be replaced by the inherent, but usually smaller, inaccuracy of daily ring counts used as known age (X). A major advantage of being able to use length to age larvae is that large sample sizes can be managed without the need to kill the sampled larva. Importantly, the period of growth stagnation after the end of the mixed feeding period needs to be considered when estimating larval age using length (Figure 7). For otolith diameters, no such stagnation was observed, and the accuracy of the age estimation was also better. The trade-off when using otolith diameters instead of larval length is increased effort and the need to kill the sampled larvae.

References

Abbas, L., and Whitfield, T. T., 2010. The zebrafish inner ear. In Zebrafish, Vol.29 (ed. S. F. Perry, M. Ekker, A. P. Farrell and C. J. Brauner). London, UK: Academic Press: 123-171.

Alderdice, D.F., and Velsen, F.P.J., 1978. Relationship between temperature and incubation time for eggs of chinook salmon (*Oncorhynchus tshawytscha*). Journal of the Fisheries Research Board of Canada 35: 69-75.

Arlinghaus R., Mehner T., & Cowx I.G., 2002 Reconciling traditional inland fisheries management and sustainability in industrialized countries, with emphasis on Europe. Fish and Fisheries 3: 261-316.

Atkinson, D., 1996. Ectotherm life-history responses to developmental temperature. In Animals and Temperature. Phenotypic and Evolutionary Adaptation (Johnston, I. A. & Bennett, A. F., eds), pp. 183-204. Cambridge: Cambridge University Press.

Barkman, R.C., and Bengtson, D.A., 1987. The record of daily growth in otoliths of Atlantic silversides, *Menidia menidia,* from field and laboratory. Journal of Fish Biology 31: 683-695.

Beacham, T.D., and Murray, C.B., 1990. Temperature, egg size, and development of embryos and alevins of five species of Pacific salmon: a comparative analysis. Transactions of the American Fisheries Society 119: 927–945.

Blaxter, J. H. S., 1988. Pattern and variety in development. In Fish Physiology, Vol. XI (Hoar, W. S. & Randall, D. J., eds), pp. 1–58. London: Academic Press.

Blaxter, J.H.S., 1992. The effect of temperature on larval fishes. Netherlands Journal of Zoology 42: 336–357.

Brett, J.R., 1970. 3. Temperature. 3.3. Animals. 3.3.2. Fishes. In: Marine Ecology (ed. O. Kinne), Vol. 1, Pt. 1, pp. 515–573. Wiley Interscience, London.

Brothers, E.B., Mathews C.P., and Lasker R., 1976. Daily growth increments in otoliths from larval and adult fishes. Fish. Bull., U.S 74: 1-8

Brothers, E.B., 1990. Otolith Marking. American Fisheries Society Symposium 7: 183-202

Campana, S.E., 1984. Lunar cycles of otolith growth in the juvenile starry flounder, *Platichthys stellatus*. Marine Biology. 80: 239-246.

Campana, S. E., and Neilson J. D., 1985. Microstructure of Fish Otoliths. Canadian Journal of Fisheries and Aquatic Sciences 42: 1014-1032.

Campana S.E., 2004. Photographic atlas of fish otoliths of the northwest Atlantic Ocean. Canadian Special Publication of Fisheries and Aquatic Sciences 133: 1-284.

Campana, S.E., and Thorrold, S.R., 2001. Otoliths, increments and elements: keys to a comprehensive understanding of fish populations? Canadian Journal of Fisheries and Aquatic Sciences 58: 30-38.

Casselman, J.M., 1987. Determination of age and growth. In The Biology of Fish Growth. Chap.7. Edited by A.H. Weatherley and H.S. Gill. Academic Press, New York. p. 209-242.

Chang, C., Lin, C., Chen, Y., Chen, M., & Chang, S., 2012. Age validation, growth estimation and cohort dynamics of the bony flying fish *Hirundichthys oxycephalus* off eastern Taiwan. Aquatic Biology 15: 251-260.

Coggins, L. G., Gwinn D. C., and Allen M. S., 2013. Evaluation of age–length key sample sizes required to estimate fish total mortality and growth. Transactions of the American Fisheries Society 142: 832-840.

Collares-Pereira, M.J., Cowx, I.G., and Coelho, M.M., 2002. Conservation of Freshwater Fish: Options for the Future. Fishing News Books, Blackwell Science, Oxford, 472pp.

Cossins, A. R., & Bowler, K., 1987. Temperature Biology of Animals. London: Chapman & Hall.

Cowx, I. G., and Gerdeaux, D., 2004. The effects of fisheries management practises on freshwater ecosystems. Fisheries Management and Ecology, 11: 145-151.

Escot, C., & Granado-Lorencio, C., 1998. Morphology of the otoliths of Barbus sclateri (Pisces: Cyprinidae). Journal of Zoology 246: 89–94.

Fossum, P., Kalish, J., and Moksness, E., 2000. 2nd International Symposium on Fish Otolith Research and Application, Bergen, Norway, 20-25 June 1998. Fisheries Research 46: 1-371

Gartner, J.V., 1991. Life histories of three species of lantern fishes (Pisces: Myctophidae) from the eastern Gulf of Mexico. I. Morphological and microstructural analysis of sagittal otoliths. Marine Biology 111: 11-20.

Gao, Y., Li, Z., Qiao, L., Ren, D., & Feng, Q., 2009. Raman and FTIR characteristics of otolith of ornamental carp. Spectroscopy and Spectral Analysis 29: 2689-2693.

Gauldie, R.W., Radtke, R.L., 1990. Microincrementation facultative and obligatory precipitation of otolith crystal. Comparative Biochemistry and Physiology 97A: 137-144

Geffen, A.J., 1996. Effect of experimental manipulation of feeding conditions on the population structure of larval Cod (Gadus morhua) and Herring (Clupea harengus). Marine and Freshwater Research 47: 291-300.

Günther, C.C., Temming, A., Baumann, H., Huwer, B., Möllmann, C., Clemmesen, C., Herrmann, J.P., 2012. A novel length back-calculation approach accounting for onto- genetic

changes in the fish length – otolith size relationship during the early life of sprat (Sprattus sprattus). Canadian Journal of Fisheries and Aquatic Sciences 69 (7): 1214-1229.

Haddon, C., and Lewis, J., 1996. Early ear development in the embryo of the Zebrafish, *Danio rerio*. Journal of Comparative Neurology 365: 113-128

Hayashi, A., Yamashita, Y., Kawaguchi, K., & Ishii, T., 1989. Rearing method and daily otolith ring of Japanese sardine larvae. Nippon Suisan Gakkaishi 55: 997-1000.

Jenkins, G., 1987. Age and growth of co-occurring larvae of two flounder species, *Rhombosolea tapirina* and *Ammotretis rostratus.* Marine Biology 95: 157-166.

Joh, M., Joh, T., Matsu-ura, T., & Takatsu, T., 2008. Validation of otolith increment formation and the growth rate of fat greenling larvae. Aquaculture Science 56: 157-166.

Joh, M., Matsuda, T., Satoh, N., Tanaka, N., & Ueda, Y., 2011. Otolith microstructure of brown sole *Pseudopleuronectes herzensteini*: validation of daily ring formation and the occurrence of microstructure denoting metamorphosis. Fisheries Science 77: 773-783.

Joh, M., Matsuda, T., and Miyazono, A., 2014. Common otolith microstructure related to key early life-history events in flatfishes identified in the larvae and juveniles of cresthead flounder *Pseudopleuronectes schrenki*. Journal of Fish Biology, 86: 448-462.

Karakiri, M., Berghahan, R.B., Von Westernhagen, H., 1989. Growth differences in O-group plaice *Pleuronectes platessa* as revealed by otolith microstructure analysis. Marine Ecology-Progress Series 74: 137-159.

Kamler, E., 1992. Early Life History of Fish: an Energetics Approach, 255 pp. Chapman and Hall, London.

Kamler, E., Keckeis, H., & Bauer-Nemeschkal, E., 1998. Temperature-induced changes of survival, development and yolk partitioning in *Chondrostoma nasus*. Journal of Fish Biology 53: 658-682.

Keckeis, H., Bauer-Nemeschkal, E., Menshutkin, V.V., Nemeschkal, H.L., Kamler, E., 2000. Effects of female attributes and egg properties of offspring viability in a rheophilic cyprinid, *Chondrostoma nasus*. Canadian Journal of Fisheries and Aquatic Sciences 57: 789-796.

Keckeis H., Kamler E., Bauer-Nemeschkal E. & Schneeweiss K. 2001. Survival, development and food energy partitioning of nase larvae and early juveniles at different temperatures. Journal of Fish Biology 59, 45–61.

Kristensen, P. B., Closs, G. P., Lokman, P. M., and Grønkjær, P., 2008, Otolith formation, microstructure and daily increment validation in juvenile perch *Perca fluviatilis*. Journal of Fish Biology 73: 1478-1483.

Kováč, V., 2000. Early development of *Zingel streber*. Journal of Fish Biology 57: 1381-1403.

Kulczykowska, E., Popek, W., & Kapoor, B. G., 2010. Biological clock in fish. Enfield, NH: Science Publishers.

Lelek, A., 1987. The freshwater fishes of Europe. Vol. 9. Aula Verlag, Wiesbaden.

Lenaz, D., Hiletic, M., Pizzul, E., Vanzo, S., & Adami, G., 2006. Mineralogy and geochemistry of otoliths in freshwater fish from northern Italy. European Journal of Mineralogy 18: 143-148.

Li, Z., Gao, Y., & Feng, Q., 2009. Hierarchical structure of the otolith of adult wild carp. Materials Science and Engineering C 29: 919-924.

Löffler, J., Ott, A., Ahnelt, H., & Keckeis, H., 2008. Early development of the skull of *Sander lucioperca* (L.) (Teleostei: Percidae) relating to growth and mortality. Journal of Fish Biology 72: 233-258.

Lucas, M.C., and Marmulla, G., 2000. An assessment of anthropogenic activities on and rehabilitation of river fisheries: current state and future direction. In: Management and Ecology of River Fisheries (ed. I.G.Cowx). Fishing News Books, Blackwell Science, Oxford, pp. 261–278.

Macdonald, J. I., McNeil, D. G., and Crook, D. A., 2012. Asteriscus v. lapillus: comparing the chemistry of two otolith types and their ability to delineate riverine populations of common carp *Cyprinus carpio*. Journal of Fish Biology, 81: 1715-1729.

Mann, D.A., Higgs, D.M., Tavolga, W.N., Souza, M.J., Popper, A.N., 2001. Ultrasound detection by clupeiform fishes. Journal of the Acoustical Society of America 109: 3048-3054.

Marshall, S.L., and Parker, S.S., 1982. Pattern identification in the microstructure of sockeye salmon (*Oncorhynchus nerka*) otoliths. Canadian Journal of Fisheries and Aquatic Sciences 39: 542-547.

Miller, S.J., and Storck, T., 1982. Daily growth rings in otoliths of young-of-the-year largemouth bass. Transactions of the American Fisheries Society 111: 527-530.

Modin, J., Fagerholm, B., Gunnarsson, B., Pihl, L., 1996. Changes in otolith microstructure at metamorphosis of plaice, *Pleuronectes platessa* L. ICES Journal of Marine Science 53: 745-748.

Morales-Nin, B., 2000. Review of the growth regulation processes of otolith daily increment formation. Fisheries Research 46 (1-3): pp. 53-67.

Mosegaard, H., Steffner, N.G., Ragnarsson, B., Manipulation of otolith microstructure as a means of mass-marking salmonid yolk sac fry, Proceedings of the Fifth Congress of European Ichthyologists 1987: pp. 213-220.

Mosegaard, H., Svedang, H., and Taberman, K., 1988. Uncoupling of somatic and otolith growth-rates in arctic char (*Salvelinus alpinus*) as an effect of differences in temperature response. Canadian Journal of Fisheries and Aquatic Sciences 45 (9): 1514-1524.

Mugiya, Y., 1987. Phase difference between calcification and organic matrix formation in the diurnal growth of otoliths in the rainbow trout, *Salmo gairdneri.* Fisheries Bulletin 85: 395-401.

Munk, K.M., Smoker, W.W., Beard, D.R., Mattson, R.W., 1993. A hatchery water-heating system and its application to 100% thermal marking of incubating salmon. The Progressive Fish-Culturist 55: 284-288.

Narimatsu, Y., Hattori, T., Ueda, Y., Matsuzaka, H., and Shiogaki, M., 2007. Somatic growth and otolith microstructure of larval and juvenile Pacific cod *Gadus macrocephalus*. Fisheries Science, 73: 1257-1264.

Ojanguren, A.F., Reyes-Gavilan, F.G., Rodriguez Munoz, R., 1999. Effects of temperature on growth and efficiency of yolk utilization in eggs and pre-feeding larval stages of Atlantic salmon. Aquaculture International 7: 81-87.

Ojanguren, A. F., and Braña, F., 2003, Thermal dependence of embryonic growth and development in brown trout. Journal of Fish Biology, 62: 580-590.

Otterlei, E., Folkvord, A., and Nyhammer, G., 2002. Temperature dependent otolith growth of larval and early juvenile Atlantic cod (*Gadus morhua*). – ICES Journal of Marine Science, 59: 401-410

Pannella, G., 1971. Fish otoliths: daily growth layers and periodical patterns. Science 173: 1124-1127

Plachta, D.T.T., Popper, A.N., Evasive responses of American shad (*Alosa sapidissima*) to ultrasonic stimuli. Acoustics Research Letters Online 4 2003: pp. 25-30.

Platt, C., Popper, A.N., 1981. Structure and function in the ear. In: Tavolga, W.N., Popper, A.N., Fay, R.R. (Eds.), Hearing and Sound Communication in Fishes. Springer, New York: pp. 3-38.

Platt, C., 1983. The peripheral vestibular system in fishes. In Northcutt, R.G., Davis, R.E. (Eds.), Fish Neurobiology. University of Michigan Press, Ann Arbor, MI: pp. 89-124

Parsons, G.R., and Peters, K.M., 1989. Age determination in larval and juvenile sheepshead, *Archosargus probatocephalus*. Fisheries Bulletin U.S. 87: 985-988.

Popper, A.N., Fay, R.R., 1993. Sound detection and processing by fish: critical review and major research questions. Brain, Behavior and Evolution. 41: 14-38.

Popper, A.N., Platt, C., 1993. Inner ear and lateral line of bony fishes. In: Evans, D.H. (Ed.), The Physiology of Fishes. CRC Press, Boca Raton, FL: pp. 99-136

Popper, A. N., & Lu, Z., 2000. Structure-function relationships in fish otolith organs. Fisheries Research 46: 15-25.

Popper, A.N., and Fay, R.R., 2011 Rethinking sound detection by fishes. Hearing Research 273: 25-36.

Raat, A.J.P., 2001 Ecological rehabilitation of the Dutch part of the River Rhine with special attention to the fish. Regulated Rivers: Research and Management 17: 131-144.

Retzius, G., 1881. Das Gehörorgan der Wirbelthiere, vol. 1. Samson and Wallin, Stockholm.

Rombough, P.J., 1988. Respiratory gas exchange, aerobic metabolism, and effects of hypoxia during early life. In Fish Physiology (eds. S. Hoar and D.J. Randall) Vol. XIA: pp. 59-61. Academic Press, San Diego.

Schludermann, E., Keckeis, H., Nemeschkal, H.L., 2009. Effect of initial size on daily growth and survival in freshwater *Chondrostoma nasus* larvae: A field survey. Journal of Fish Biology 74: 939-955.

Secor, D.H., Dean, J.M., and Campana, S.E., (Editors). 1995. Recent developments in fish otolith research. University of South Carolina Press, Columbia, SC. 735 p.

Souchon, Y., and Keith, P., 2001. Freshwater fish habitat: science, management and conservation in France. Aquatic Ecosystem Health and Management 4: 401-412.

Campana, S. E., and C. M. Jones. 1992. Analysis of otolith microstructure data. Pages 73-100 in D. K. Stevenson and S. E. Campana [ed.] Otolith microstructure examination and analysis. Can. Spec. Publ. Fish. Aquat. Sci. 117. 126 p.

Stooke-Vaughan, G. A., Huang, P., Hammond, K. L., Schier, A. F., & Whitfield, T. T., 2012. The role of hair cells, cilia and ciliary motility in otolith formation in the zebrafish otic vesicle. Development (Cambridge, England), 139(10): 1777-1787.

Summerfelt, R.C., and Hall, G.E., (Editors) 1987. Age and growth of fish. Iowa State University Press, Ames, IA. 544 p.

Tsuji, S., & Aoyama, T., 1984. Daily growth increments in otolith of Japanese anchovy larvae *Engraulis japonica.* Nippon Suisan Gakkaishi 50: 1105-1108.

Volk, E.C., Schroder, S.L., Fresh, K.L., 1990. Inducement of unique otolith banding patterns as a practical means to mass-mark juvenile pacific salmon. American Fisheries Society Symposium 7: 203-215.

Volk, E.C., Schroder, S.L., Grimm, J.J., Ackley, H.S., 1994. Use of a bar code symbology to produce multiple thermally induced marks. Transactions of the American Fisheries Society. 123: 811-816.

Volk, E. C., and Hagen, P., 2001. An Overview of Thermal Marking. NPAFC Technical Report No. 3

Whitmore, D., Foulkes, N. S., Strähle, U., & Sassone-Corsi P., 1998. Zebrafish Clock rhythmic expression reveals independent peripheral circadian oscillators. Nature Neuroscience 1: 701-707.

Wolter, C., 2001) Conservation of fish species diversity in navigable waterways. Landscape and Urban Planning 53, 135–144.

Wu, D., Freund, J. B., Fraser, S. E., Vermot, J., 2011. Mechanistic Basis of Otolith Formation during Teleost Inner Ear Development. Dev Cell 20: 217-278.

Yamada, H., Chimura, M., Asami, K., Sato, T., Kobayashi, M. & Nanami, A., 2009. Otolith development and daily increment formation in laboratory-reared larval and juvenile black-spot tuskfish *Choerodon schoenleinii.* Fisheries Science 75: 1141-1146.

Yang, L., Li, S. R. & Luo, J. Y., 2009. Study on $CaCO_3$ crystal structure and its environmental information of carp asteriscus from Miyun Reservoir and Baiyangdian Lake. Goldschmidt Conference Abstracts 2009, A1476.

Yúfera, M., Darias, M.J., 2007. The onset of exogenous feeding in marine fish larvae. Aquaculture 268: 53-63.

Zhang, Z. and Runham, N. W., 1992. Otolith microstructure pattern in *Oreochromis niloticus* (L.). Journal of Fish Biology, 40: 325-332.

Acknowledgements

I would like to thank Hubert Keckeis for his great supervision and help, not only with this thesis but throughout my Master's studies. My colleagues Aaron Lechner, Franz Lumesberger-Loisl, David Ramler, Maximilian Sehr, Astrid Toth and Holger Villwock for their advice and the good times during field work.
Special thanks to Michael Stachowitsch for improving the English and the FWF for funding the project (MODI P22631-B17 "Modelling dispersal patterns of fish larvae in a large river") of which this thesis is a part.